Triptycene-grafted helicenes: modular synthesis and key properties

Supporting Information

Pattarakiat Seankongsuk, Martin Vacek, Jiří Rybáček, Jaroslav Vacek, Katsiaryna Kutsenka, Lucie Bednárová, Radek Pohl, Ivana Císařová, Irena G. Stará* and Ivo Starý*

Table of Contents

Experimental section (General)

Melting points were determined on Mikro-Heiztisch Polytherm A (Hund, Wetzlar) apparatus and are uncorrected.

The NMR spectra were measured on Bruker Advance III HD 400, 500 and 600 MHz instruments, respectively, or JEOL JNM-ECZR 500 MHz in $CDCl_3$, $C_2D_2Cl_4$ or THF-d_8 as indicated in 5 mm PFG probe with indirect detection. NMR spectra were referenced using the residual signals of solvents. The chemical shifts are given in δ-scale, the coupling constants J are given in Hz. For the correct assignment of both the ^{1}H and ^{13}C NMR spectra of key compounds, homonuclear 2D-H,H-COSY, 2D-H,H-ROESY and heteronuclear 2D-H,C-HSQC and 2D-H,C-HMBC experiments were performed.

The ESI mass spectra were recorded using a quadrupole orthogonal acceleration time-of-flight tandem mass spectrometer (Q-Tof micro, Waters) and high-resolution ESI mass spectra using a hybrid FT mass spectrometer combining a linear ion trap MS and the Orbitrap mass analyser (LTQ Orbitrap XL, Thermo Fisher Scientific). The conditions were optimised for suitable ionisation in the ESI Orbitrap source (sheath gas flow rate 35 a.u., aux gas flow rate 10 a.u. of nitrogen, source voltage 4.3 kV, capillary voltage 40 V, capillary temperature 275 °C, tube lens voltage 155 V). The samples were dissolved in methanol and applied by direct injection. As mobile phase was used 80% methanol (flow rate 100 µl/min). The MALDI-TOF spectra were measured on UltrafleXtremeTM MALDI-TOF/TOF mass spectrometer (Bruker Daltonics, Germany) with 1 kHz Smartbeam II laser using Dried Droplet technique with 2,5-DHB as matrix. The measurements were done in a positive reflectron mode technique. The accelerating voltage was set at 20kV.

The ECD, absorption and fluorescence spectra were measured on a Jasco 1500 spectropolarimeter (JASCO International Co. Ltd.) equipped with a fluorescence emission monochromator (FMO522) and separate fluorescence emission detector (FDT-538). The ECD and absorption spectra were measured over a spectral range of 210 nm to 600 nm in tetrahydrofuran solutions (10^{-4} M). Measurements were made in quartz cell with a 0.2 cm path length using a scanning speed of 20 nm/min, a response time of 4 seconds, one accumulation and standard instrument sensitivity. After a baseline correction, spectra were expressed in terms of differential molar extinction (Δε) and molar extinction (ε), respectively. Fluorescence spectra were measured in tetrahydrofuran (10^{-5} M and 10^{-6} M (not presented)) with emission and excitation slits 10 nm and 5 nm, respectively, with excitation wavelength indicated in the spectra. Spectra of circularly polarised luminescence (CPL) were acquired on Jasco CPL-300 instrument (JASCO International Co. Ltd.) over a spectral range of 350 nm to 700 nm in tetrahydrofuran or toluene (10^{-5} M) using the following setup (for measurements in tetrahydrofuran): quartz cell with 1 cm path length, excitation and emission slits 2000 µm and 1500 µm, respectively, scanning speed of 10 nm/min, response time of 8 s, 3 accumulations, and an excitation wavelength of 286 nm (for compound **2**) or 282 nm (for

compound **3**). For compound **3** in toluene, scanning speed of 5 nm/min and response time of 16 s with 10 accumulations were used.

Lifetimes of fluorescence were measured by TCSPC on Fluoromax-4 (Horiba) equipped with a nanoled excitation light source (368 nm) and a PMT detector in THF and toluene (10^{-5} M) over 200 ns range using the repetition frequency of 1 MHz and 1 nm optical slits. For prompt measurements, a dilute dispersion of Ludox in MilliQ water was used. Fluorescence lifetime decays were analyzed using a forward convolution fit based on the Maximum Likelihood Estimation (MLE) method, minimizing the Poisson deviance (C-statistic). The experimental intensity decay, I(t), was modeled as the convolution of the instrument response function, IRF(t), with a multi-exponential decay function, accounting for a wavelength-dependent time shift (δ) and a contribution from scattered light (A_{scat}):

$$I(t) = IRF(t-\delta) \otimes \left(\sum_{i=1}^{n} \alpha_i e^{-\frac{t}{\tau_i}} \right) + A_{scat} IRF(t-\delta) + B$$

where τ_i and α_i are the lifetime and amplitude of the *i*-th decay component, respectively, δ represents the color shift (IRF shift) between the excitation and emission wavelengths, A_{scat} is the amplitude of the scatter contribution (Rayleigh/Raman), and B is the constant background. The fractional intensity contribution of each species was calculated as $f_i=(\alpha_i\tau_i)/\sum(\alpha_j\tau_j)$. Parameter uncertainty was determined via parametric bootstrapping (N=1000 iterations). Synthetic decays were generated by applying Poisson noise to the best-fit model and re-analyzed; reported errors correspond to the 16th–84th percentile interval of the bootstrap distribution. Goodness-of-fit was assessed using the reduced chi-squared value (χ_{red}^2) and the distribution of weighted residuals

The IR spectra were measured in $CHCl_3$ in KBr cell (0.1 mm pathlength) using a Nicolet 6700 or a Nicolet is50 instrument. Optical rotations were measured in $CHCl_3$ using an Autopol IV instrument (Rudolph Research Analytical).

For analytical separations (*e.g.* determination of enantiomeric excess), an UHPSFC/MS system was used (Waters UPC^2) with a mixture of CO_2 (99.995%) and 1% *i*-PrOH in DCM as mobile phase (flow rate = 1.5 ml/min, temperature = 35 °C, backpressure = 2000 psi) and Alcyon ChiralArt Amylose-SA (150 x 3 mm ID, 3 µm, YMC) as the CSP column. Chromatographic data were acquired with a diode array UV detector (210 - 400 nm) using MassLynx software. For DHPLC experiments, Knauer Azura binary high-pressure gradient HPLC instrument equipped with a DAD (200-800 nm) detector and a Peltier-cooled column thermostat was used. Semipreparative resolutions were then performed on an Interchim PuriFlash P5.250 HPFC/HPLC system equipped with a DAD (200-800 nm) detector using ChiralArt Amylose-SA (250 x 20 mm ID, 5 µm, YMC) as the CSP column and a gradient from

50 to 100% toluene in heptane at 20 mL/min. as an eluent. Samples (cca 10 mg) were dissolved in toluene (cca 1 mL) and filtered through a hydrophobic PTFA membrane filter (0.23 µm) before injection.

TLC was performed on Silica gel 60 F254-coated aluminium sheets (Merck) and spots were detected by the solution of $Ce(SO_4)_2.4\,H_2O$ (1%) and $H_3P(Mo_3O_{10})_4$ (2%) in sulfuric acid (10%). The flash chromatography was performed on Silica gel 60 (0.040-0.063 mm, Merck) using Isolera One HPFC system (Biotage, Inc.).

Biotage Initiator+ (400 W power) was used for reactions carried out in a microwave reactor. Microwave reactions were performed in crimp-sealed reaction vessels.

Tetrahydrofuran was freshly distilled from sodium/benzophenone under nitrogen; toluene was freshly distilled from sodium under nitrogen. Diisopropylamine was distilled from calcium hydride under nitrogen and degassed by three freeze-pump-thaw cycles before use. Otherwise, all commercially available solvents, catalysts and reagent grade materials were used as received. The starting compounds **4** and **5** are commercially available, compound **6** was prepared according to a literature procedure,[1] as were alkynes **9**,[2] **12**,[3] **15**[2] and parent [n]helicenes[4] (n = 5, 6, 7) **18**–**20**.

[1] L. Ueberricke, J. Schwarz, F. Ghalami, M. Matthiesen, F. Rominger, S. M. Elbert, J. Zaumseil, M. Elstner and M. Mastalerz, *Chem. Eur. J.*, 2020, **26**, 12596–12605.

[2] H.-K. Chang, S. Datta, A. Das, A. Odedra, R.-S. Liu, *Angew. Chem. Int. Ed.* 2007, **25**, 4744-4747.

[3] A. Jančařík, J. Rybáček, K. Cocq, J. Vacek Chocholoušová, J. Vacek, R. Pohl, L. Bednárová, P. Fiedler, I. Císařová, I. G. Stará, I. Starý, *Angew. Chem. Int. Ed.* 2013, **125**, 10154-10159.

[4] F. Teplý, I. G. Stará, I. Starý, A. Kollárovič, D. Šaman. L. Rulíšek, P. Fiedler, *J. Am. Chem. Soc*. 2002, **124**, 9175–9180.

Synthesis of boronic acid 8

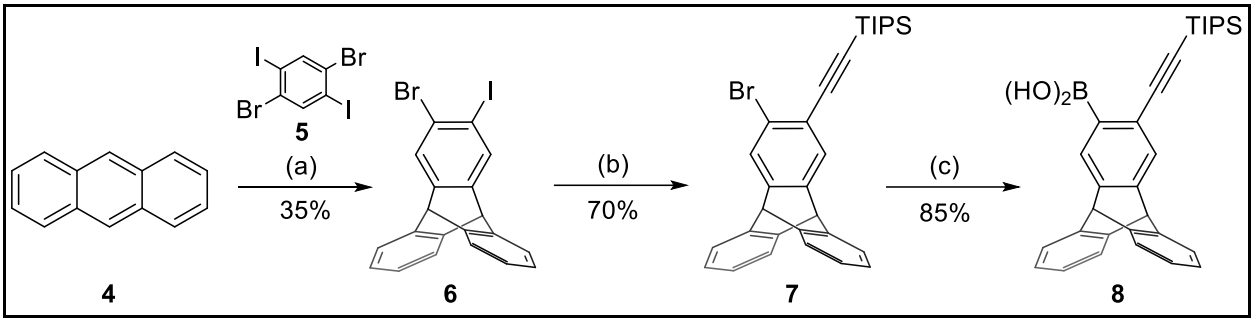

(a) 1,4-Dibromo-2,5-diiodobenzene **5** (1.7 equiv.), *n*-BuLi (1.7 equiv.), toluene, 0 °C to rt, 20 h, 41%; (b) (triisopropylsilyl)acetylene (1.7 equiv.), $Pd(PPh_3)_2Cl_2$ (3 mol%), CuI (6 mol%), toluene-DIPA (1 : 1), 35 °C, 1 h, 70%; (c) *n*-BuLi (1.6 equiv.), THF, - 78 °C, 30 min, then triisopropyl borate (2.4 equiv.), -78 °C to rt, 2 h, then HCl (2 M, aq.), rt, 1 h, 85%.

2-Bromo-3-iodo-9,10-dihydro-9,10-[1,2]benzenoanthracene 6

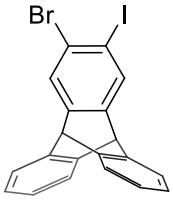

Triptycene derivative **6** was prepared by modification of a literature protocol.[1] In a Schlenk flask, anthracene **4** (0.400 g, 2.24 mmol) and 1,4-dibromo-2,5-diiodobenzene **5** (1.90 g, 3.90 mmol, 1.7 equiv.), both commercially available, were dissolved in distilled toluene (35 mL) under nitrogen atmosphere. A solution of *n*-BuLi in hexanes (1.55 M, 2.50 mL, 3.88 mmol, 1.7 equiv.) was first diluted with distilled toluene (13 mL) at 0 °C under N_2 and then added dropwise into the reaction mixture at 0 °C over 20 min. After ten minutes at 0 °C the mixture was allowed to warm to room temperature and stirred for 20 h at the same temperature. Then, the reaction was quenched by adding water (20 mL). The mixture was extracted with EtOAc (3 x 40 mL), wash with brine (100 mL), dried over anhydrous $MgSO_4$, and evaporated under reduced pressure. The crude material was purified by column chromatography (hexane-ethyl acetate 100: 0 to 95:5) to give 2-bromo-3-iodotriptycene **6** (0.419 g, 41%) as a colourless solid. NMR spectra were in agreement with the published ones.

^{1}H NMR (400 MHz, $CDCl_3$): δ 7.87 (s, 1H), 7.65 (s, 1H), 7.38 (dd, *J* = 5.3, 3.2 Hz, 4H), 7.03 (dd, *J* = 5.4, 3.1 Hz, 4H), 5.35 (s, 2H).

^{13}C NMR (101 MHz, $CDCl_3$): δ 147.61, 146.43, 144.24, 144.20, 135.02, 127.91, 125.82, 125.78, 125.75, 124.00, 123.98, 96.60, 53.33, 53.01.

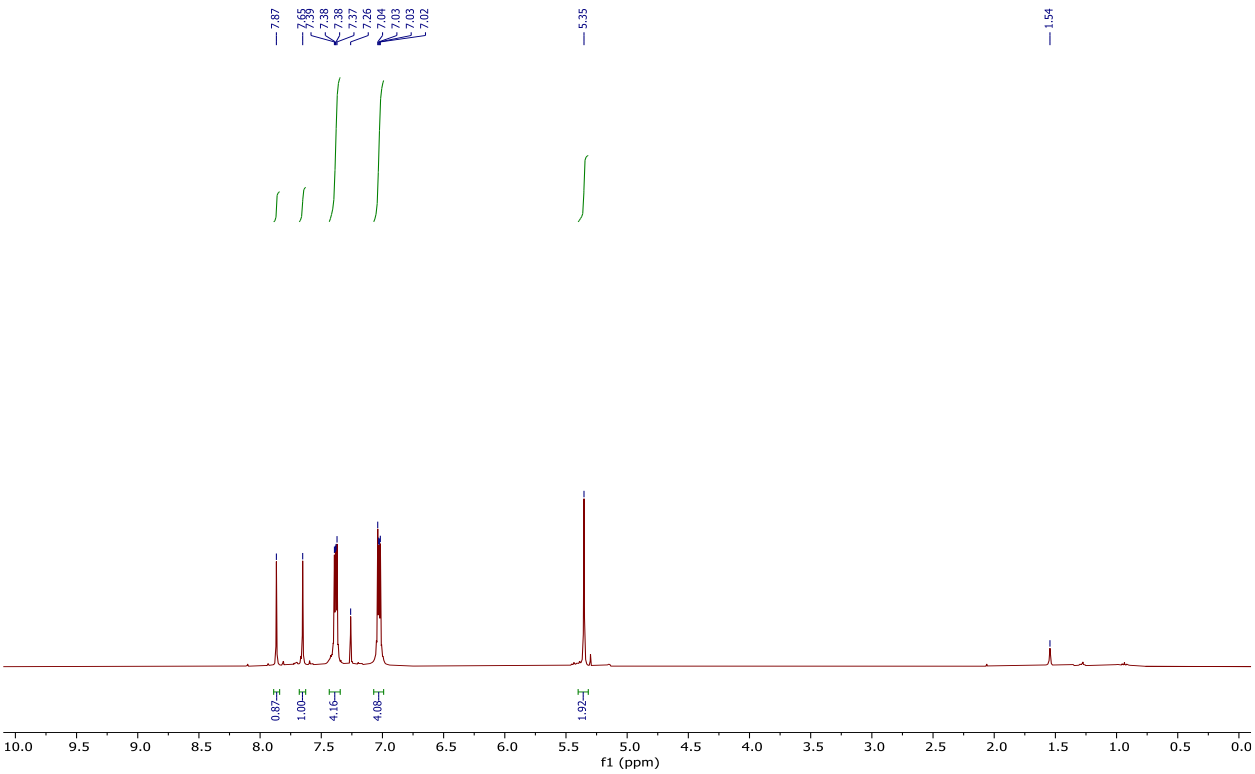

Figure S1: ^{1}H NMR of 6 (400 MHz, $CDCl_3$)

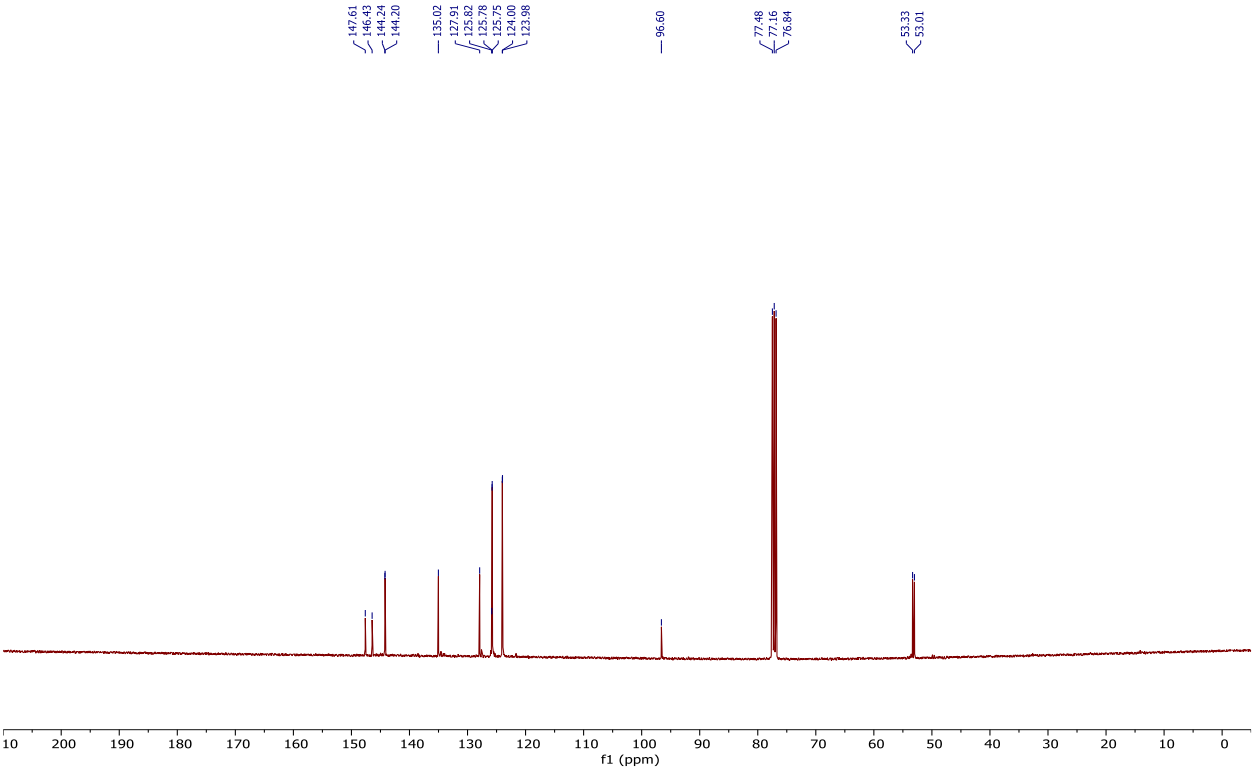

Figure S2: ^{13}C NMR of 6 (101 MHz, $CDCl_3$)

3-Bromo-9,10-dihydro-9,10-[1,2]benzenoanthracen-2-yl)ethynyl)triisopropylsilane 7

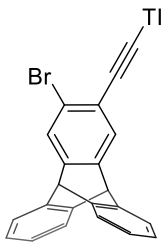

A solution of 2-bromo-3-iodotriptycene **6** (2.65 g, 5.77 mmol), $Pd(PPh_3)_2Cl_2$ (13 mg, 0.19 mmol, 3 mol%), and CuI (70 mg, 0.37 mmol, 6 mol%) in a mixture of *i*-Pr_2NH and toluene (1 : 1, 32 mL) was degassed by three cycles of freeze-pump-thaw. The mixture was stirred under nitrogen at 35 °C for 5 min. Then, (triisopropylsilyl)acetylene (2.2 mL, 9.9 mmol, 1.7 equiv.) was added dropwise into the mixture. The reaction was stirred under nitrogen at 35 °C for 1 h. After that the mixture was quenched with a saturated aqueous NH_4Cl solution (50 mL) and extracted with EtOAc (3 x 50 mL). The combined organic phase was washed with brine (100 mL), dried over anhydrous $MgSO_4$, and evaporated under reduced pressure. The crude material was pre-adsorbed on silica gel and purified by column chromatography (hexane-DCM 97:3) to obtain **7** (2.09 g, 70%) as a light-yellow solid.

^{1}H NMR (400 MHz, $CDCl_3$): δ 7.59 (s, 1H), 7.52 (s, 1H), 7.40 – 7.34 (m, 4H), 7.01 (dd, *J* = 5.4, 3.2 Hz, 4H), 5.37 (s, 1H), 5.36 (s, 1H), 1.12 (s, 21H).

^{13}C NMR (101 MHz, $CDCl_3$): δ 147.23, 144.47, 144.21, 128.67, 127.69, 125.71, 125.66, 123.95, 123.89, 122.33, 122.08, 105.24, 95.14, 53.60, 53.34, 18.80, 11.42. One signal for a quaternary carbon atom is missing, probably due to slow relaxation.

HR MS (ESI) m/z: ($[M+H]^+$) calcd for $C_{31}H_{34}{}^{79}BrSi$ 513.1608, found 513.1607 (Δ = -0.15 ppm).

IR ($CHCl_3$): 3073 w, 2960 s, 2944 s, 2927 s, 2897 m, 2866 s, 2156 w, 1959 vs, 1613 vw, 1588 vw, 1560 vvw, 1460 vs, 1454 vs, 1387 w, 1367 w, 1295 w, 1189 w, 1155 w, 1123 m, 1074 w, 1025 w, 1018 w, 997 m, 883 m, 831 m, 773 w, 710 w, 678 m, 661 m, 638 s, 616 w, 511 w cm^{-1}.

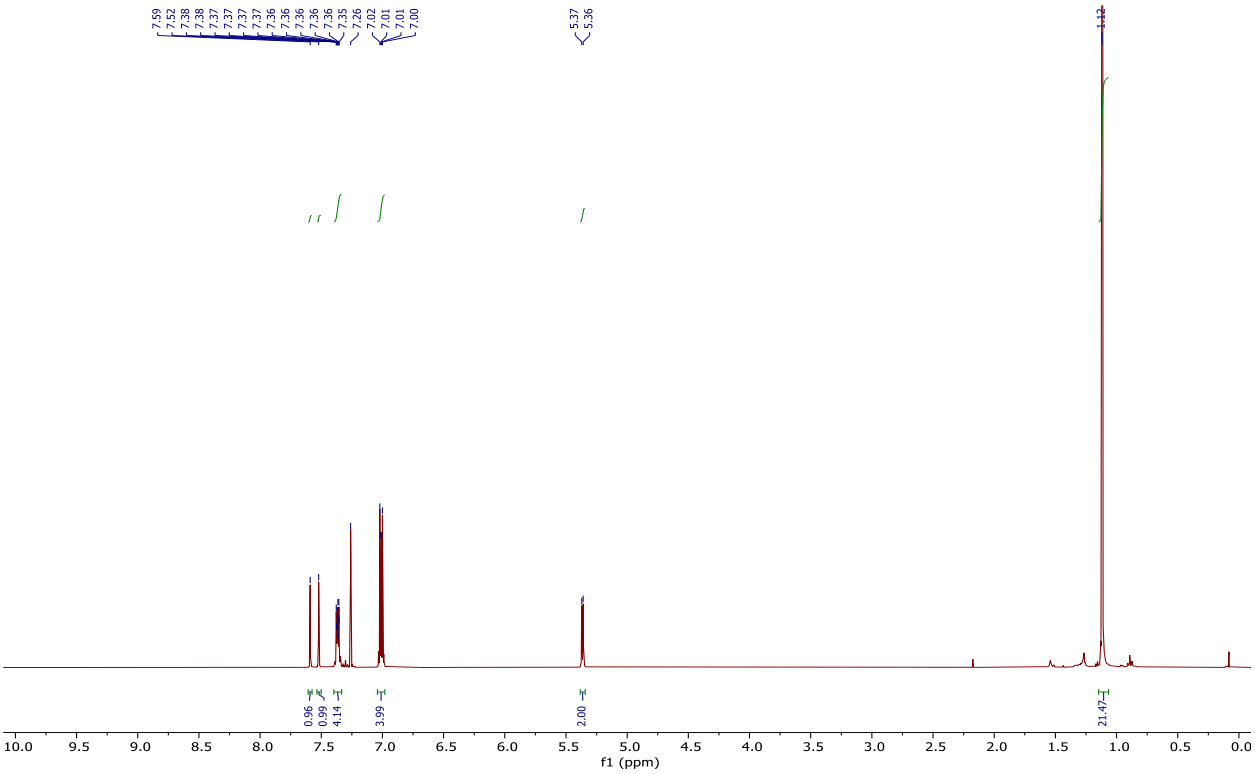

Figure S3: ^{1}H NMR of 7 (400 MHz, $CDCl_3$)

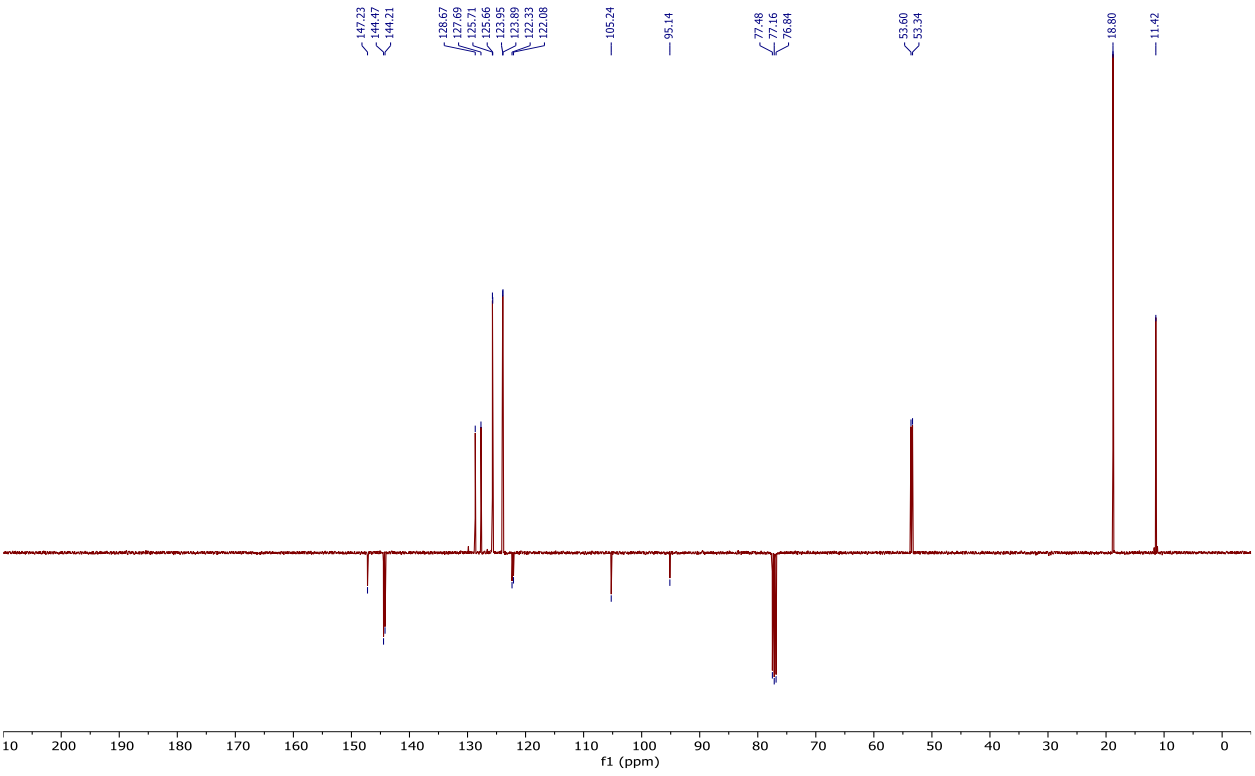

Figure S4: ^{13}C NMR of 7 (101 MHz, $CDCl_3$)

((9*s*,10*s*)-3-((Triisopropylsilyl)ethynyl)-9,10-dihydro-9,10-[1,2]benzenoanthracen-2-yl)boronic acid 8

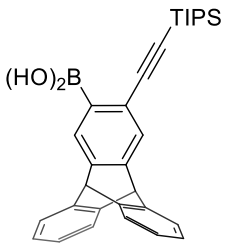

An *n*-BuLi solution (1.6 M in hexanes, 2.6 mL, 4.2 mmol, 1.6 equiv.) was added dropwise into a solution of bromo-triptycene **7** (1.31 g, 2.56 mmol) in distilled THF (17 mL) at -78 °C under nitrogen. The reaction mixture was stirred at -78 °C for 30 min. Then, triisopropyl borate (1.4 mL, 6.1 mmol, 2.4 equiv.) was added at -78 °C and stirred at the same temperature for 10 min. After that, the reaction mixture was immediately warmed up to room temperature and stirred for 2 h. Then, an aqueous HCl solution (2 M, 20 mL) was added to the reaction mixture and stirred for 1 h. The mixture was extracted with EtOAc (3 x 30 mL), the combined organic phases were washed with brine (80 mL), dried over anhydrous Na_2SO_4, and evaporated under reduced pressure. The crude material was purified by column chromatography (hexane-EtOAc 95:5 to 80:20) to obtain triptycenyl boronic acid **8** (1.04 g, 85%) as a light-yellow solid.

^{1}H NMR (400 MHz, $CDCl_3$): δ 8.01 (s, 1H), 7.58 (s, 1H), 7.40 (dd, *J* = 5.3, 3.2 Hz, 4H), 7.01 (dd, *J* = 5.4, 3.1 Hz, 4H), 5.99 (s, 2H), 5.49 (s, 1H), 5.45 (s, 1H), 1.15 (s, 21H).

^{13}C NMR (101 MHz, $CDCl_3$) δ 148.17, 145.88, 144.74, 144.34, 130.38, 128.27, 125.62, 125.50, 124.22, 123.96, 123.89, 108.89, 94.96, 54.00, 53.83, 18.73, 11.39. One signal for a quaternary carbon atom is missing, probably due to slow relaxation.

HR MS (ESI) m/z: ($[M+Na]^+$) calcd for $C_{31}H_{35}O_2BNaSi$ 501.2392, found 501.2390 (Δ = -0.25 ppm).

IR ($CHCl_3$): 3620 m, 3508 m, 3073 w, 3010 w, 2961 s, 2946 s, 2892 vs, 2867 s, 2138 m, 1614 w, 1589 w, 1547 w, 1486 w, 1460 vs, 1438 m, 1412 vs, 1370 s, 1333 m, 1155 w, 1103 w, 1072 w, 1018 w, 982 m, 883 m, 679 m, 626 s, 483 w cm^{-1}.

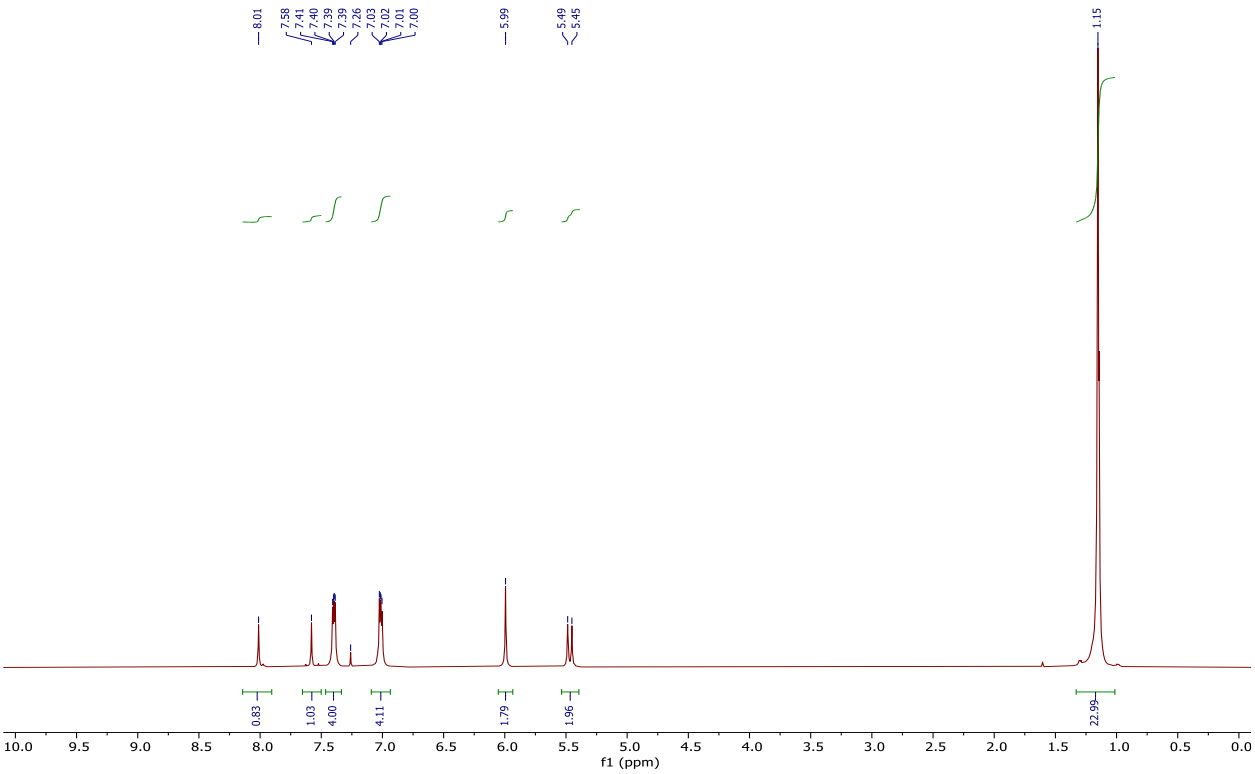

Figure S5: ^{1}H NMR of 8 (400 MHz, $CDCl_3$)

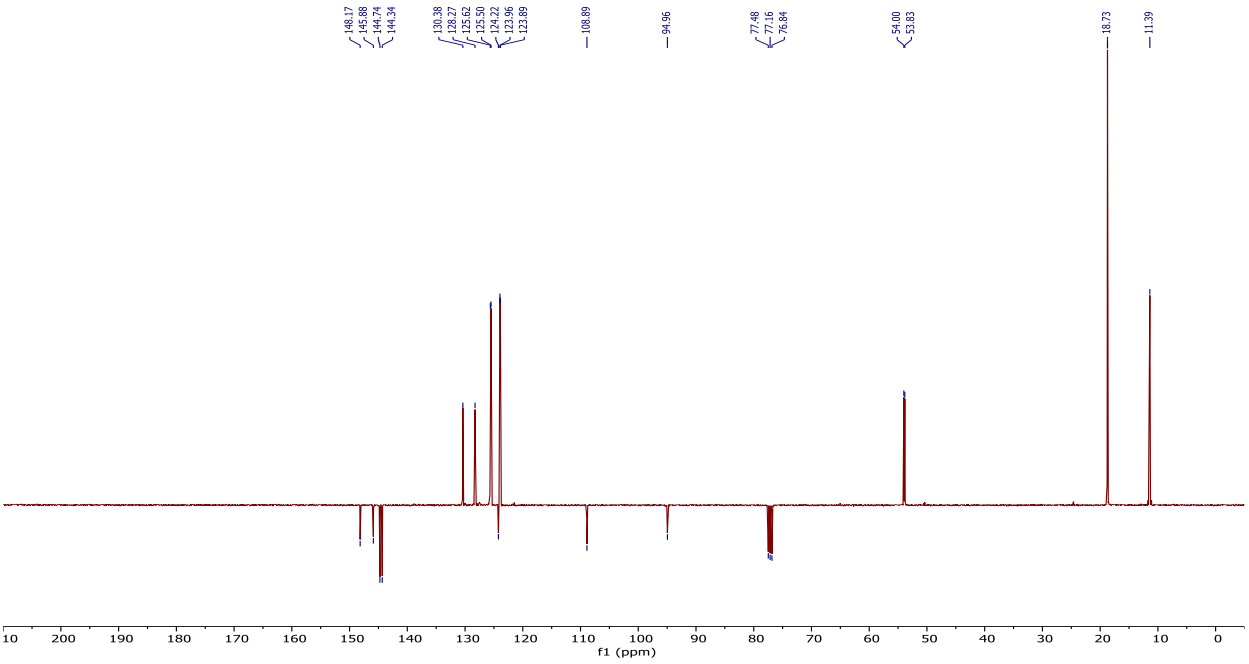

Figure S6: ^{13}C NMR of 8 (101 MHz, $CDCl_3$)

Synthesis of ditriptyceno[5]helicene 1

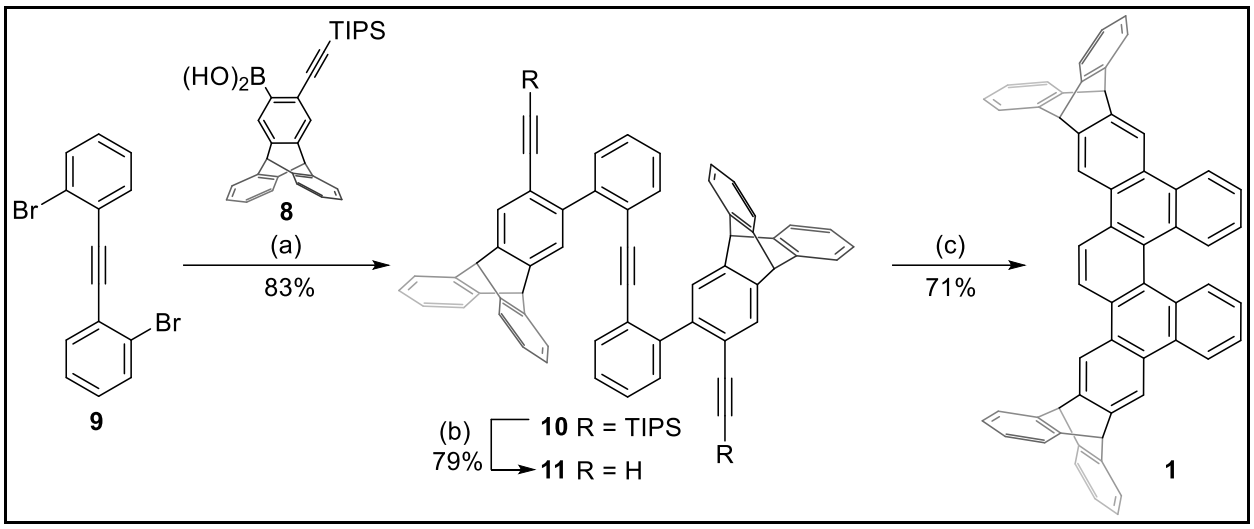

(a) Triptycenyl boronic acid **8** (2.3 equiv.), $Pd(PPh_3)_2Cl_2$ (5 mol%), Cs_2CO_3 (3.3 equiv.), toluene-EtOH-H_2O (4.3 : 4.3 : 1), 90 °C, 3 h, 83%; (b) *n*-TBAF in THF (1 M, 2.2 equiv.), THF-MeOH (100 : 1), 0 °C to rt, 1 h, 79%; (c) Wilkinson's catalyst (10 mol%), PhCl, MW, 160 °C, 20 min, 71%.

[Ethyne-1,2-diylbis(2,1-phenylenepentacyclo[6.6.6.$0^{2,7}$.$0^{9,14}$.$0^{15,20}$]icosa-2,4,6,9,11,13,15,17,19-nonaene-5,4-diylethyne-2,1-diyl)]bis(triisopropylsilane) 10

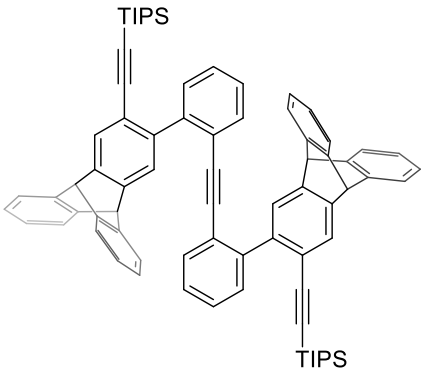

A solution of triptycenyl boronic acid **8** (29.8 mg, 62.3 µmol, 2.3 equiv.), 1,2-bis(2-bromophenyl)ethyne **9** (9.0 mg, 62 µmol), $Pd(PPh_3)_2Cl_2$ (0.9 mg, 1.3 µmol, 5 mol%), and Cs_2CO_3 (28.5 mg, 87.5 µmol, 3.3 equiv.) in a mixture of toluene-EtOH-H_2O (4.3 : 4.3 : 1, 0.8 mL) was degassed by bubbling with N_2 for 30 min. The reaction mixture was stirred at 90 °C under nitrogen for 3 h. Water (3 mL) was added to quench the reaction, and the solution was extracted with DCM (2 x 3 mL). The combined organic fractions were dried over anhydrous $MgSO_4$ and evaporated under reduced pressure. The crude material was pre-adsorbed on silica gel and purified by column chromatography (hexane-DCM 95:5 to 85:15) to obtain TIPS-protected triptycenyl triyne **10** (23.3 mg, 83%) as a colourless amorphous solid.

^{1}H NMR (400 MHz, $CDCl_3$): δ 7.66 (s, 2H), 7.59 (s, 2H), 7.52 – 7.33 (m, 10H), 7.15 (t, *J* = 7.6 Hz, 2H), 7.07 (dd, *J* = 5.4, 3.2 Hz, 8H), 6.89 (t, *J* = 7.6 Hz, 2H), 6.41 (d, *J* = 7.8 Hz, 2H), 5.50 (s, 2H), 5.46 (s, 2H), 0.95 (s, 42H).

^{13}C NMR (101 MHz, $CDCl_3$): δ 145.00 (2xC), 144.74, 144.23, 141.99, 140.37, 132.43, 130.63, 128.20, 127.23, 127.13, 125.97, 125.55, 125.43, 123.90, 123.89, 122.37, 119.42, 106.61, 92.79, 92.31, 54.05, 53.69, 18.72, 11.37.

HR MS (ESI) m/z: ($[M+Na]^+$) calcd for $C_{76}H_{74}NaSi_2$ 1065.5221, found 1065.5211 (Δ = -0.95 ppm).

IR ($CHCl_3$): 3068 w, 3008 w, 2961 s, 2944 s, 2891 m, 2865 s, 2147 w, 1597 w, 1589 w, 1460 vs, 1383 w, 1155 w, 1107 w, 1073 w, 1023 w, 997 w, 883 m, 678 m, 633 s, 481 w cm^{-1}.

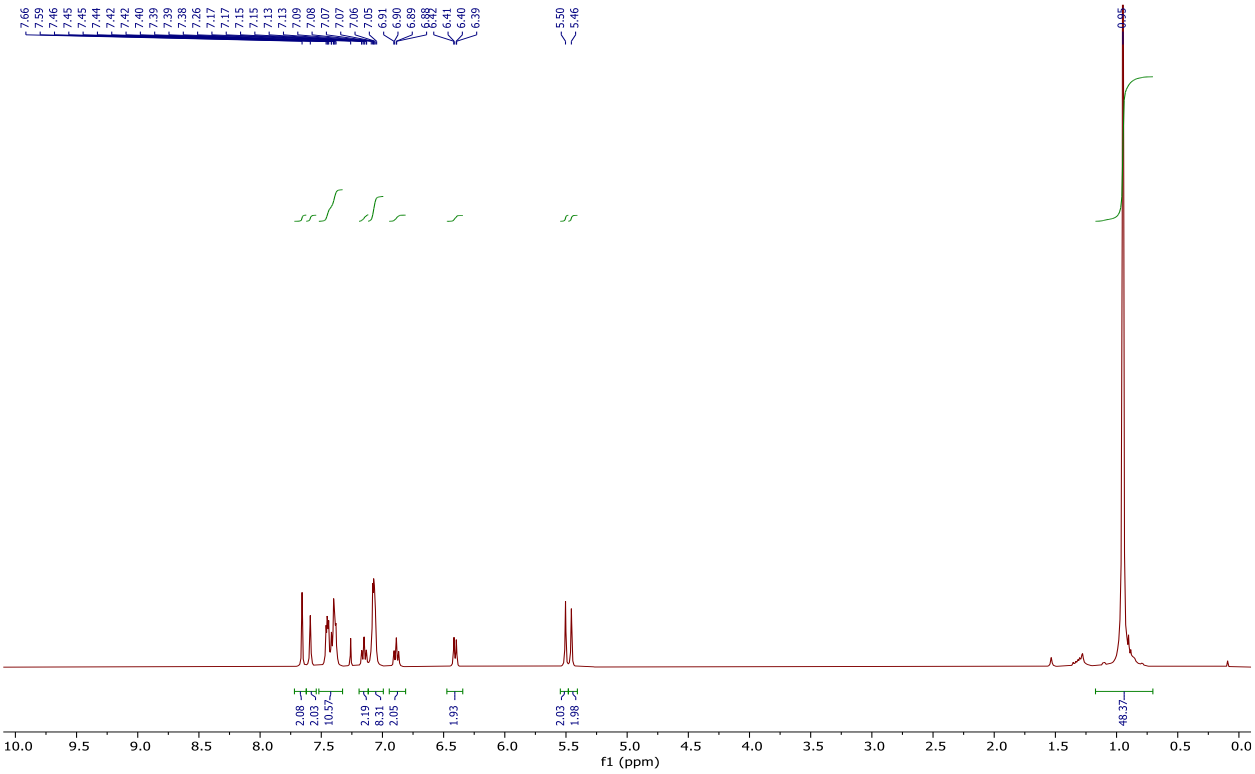

Figure S7: ^{1}H NMR of 10 (400 MHz, $CDCl_3$)

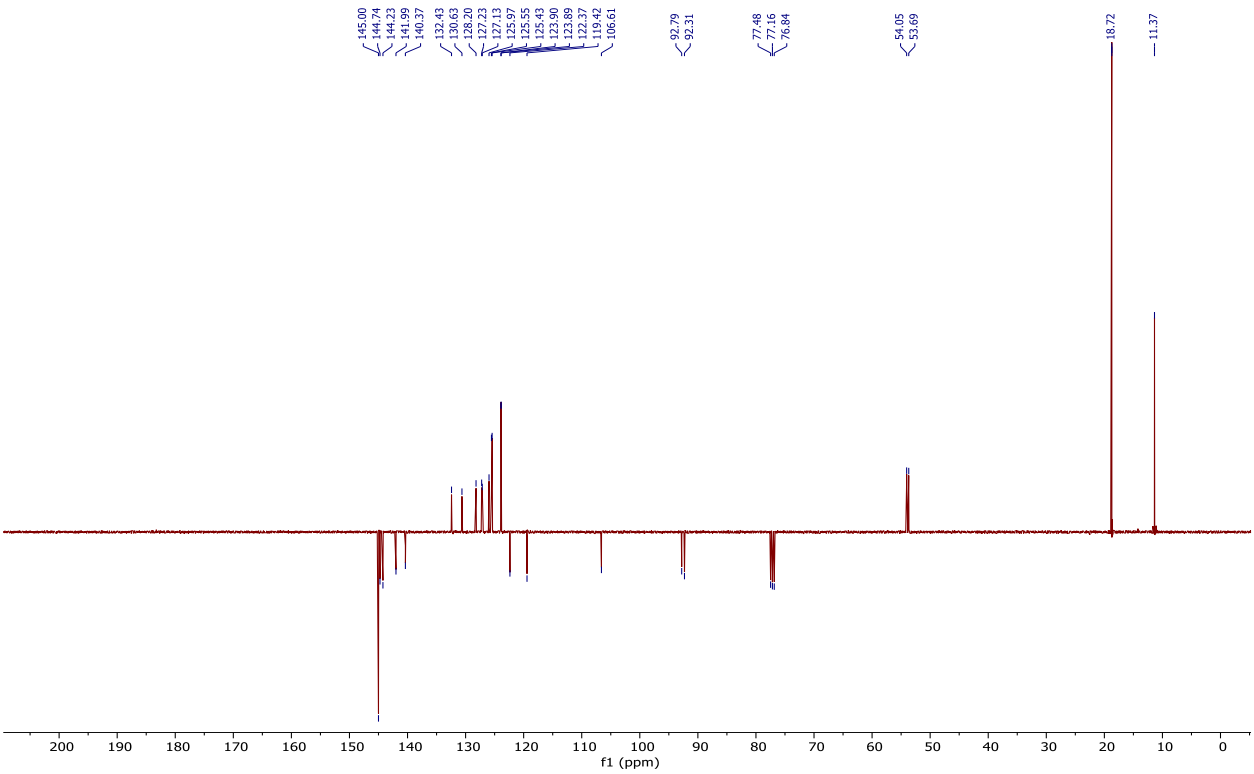

Figure S8: ^{13}C NMR of 10 (101 MHz, $CDCl_3$)

4,4'-(Ethyne-1,2-diyldi-2,1-phenylene)bis(5-ethynylpentacyclo[6.6.6.0^{2,7}.0^{9,14}.0^{15,20}]icosa-2,4,6,9,11,13,15,17,19-nonaene) 11

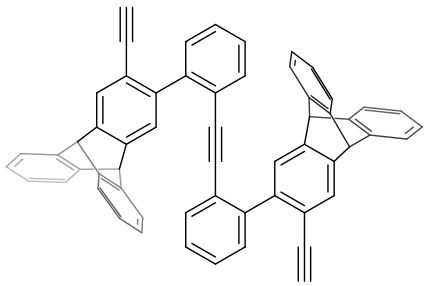

The TIPS-protected triptycenyl triyne **10** (28.5 mg, 27.3 µmol), and MeOH (6 µL) were dissolved in distilled THF (0.61 mL). An *n*-TBAF solution in THF (1 M, 60 µL, 60 µmol, 2.2 equiv.) was added dropwise at 0 °C under nitrogen. The reaction was stirred at 0 °C for 20 min. Then the mixture was warmed up to room temperature and stirred for 1 h. After that MeOH (0.5 mL) was added to quench the reaction and the resultant was stirred for further 20 min at the same temperature. The mixture was evaporated under reduced pressure and purified by column chromatography using (hexane-DCM 67:33 to 50:50 to 0:100) to obtain triptycenyl triyne **11** (15.4 mg, 79%) as a colourless amorphous solid.

^{1}H NMR (400 MHz, $CDCl_3$): δ 7.63 (s, 2H), 7.55 (s, 2H), 7.50 – 7.36 (m, 8H), 7.35 (dd, *J* = 8.1, 1.2 Hz, 2H), 7.20 (td, *J* = 7.6, 1.4 Hz, 2H), 7.07 (dd, *J* = 5.4, 3.1 Hz, 8H), 6.93 (td, *J* = 7.6, 1.3 Hz, 2H), 6.44 (dd, *J* = 7.8, 1.3 Hz, 2H), 5.49 (s, 2H), 5.48 (s, 2H), 2.79 (s, 2H).

^{13}C NMR (101 MHz, $CDCl_3$): δ 145.30, 144.95, 144.92, 144.44, 141.90, 140.69, 132.40, 130.37, 128.29, 127.40, 127.27, 126.08, 125.61, 125.49, 123.96, 123.94, 122.42, 117.89, 92.21, 83.21, 79.23, 54.00, 53.67.

HR MS (MALDI) m/z: ([M+Na]$^+$) calcd for $C_{58}H_{34}Na$ 753.2558, found 753.2560 (Δ = 0.27 ppm).

IR ($CHCl_3$): 3308 m, 3063 w, 3018 w, 2220 vw, 2102 w, 1597 w, 1587 w, 1459 vs 1447 m, 1103 w, 1023 w, 765 s, 746 vs, 477 m, 471 m cm^{-1}.

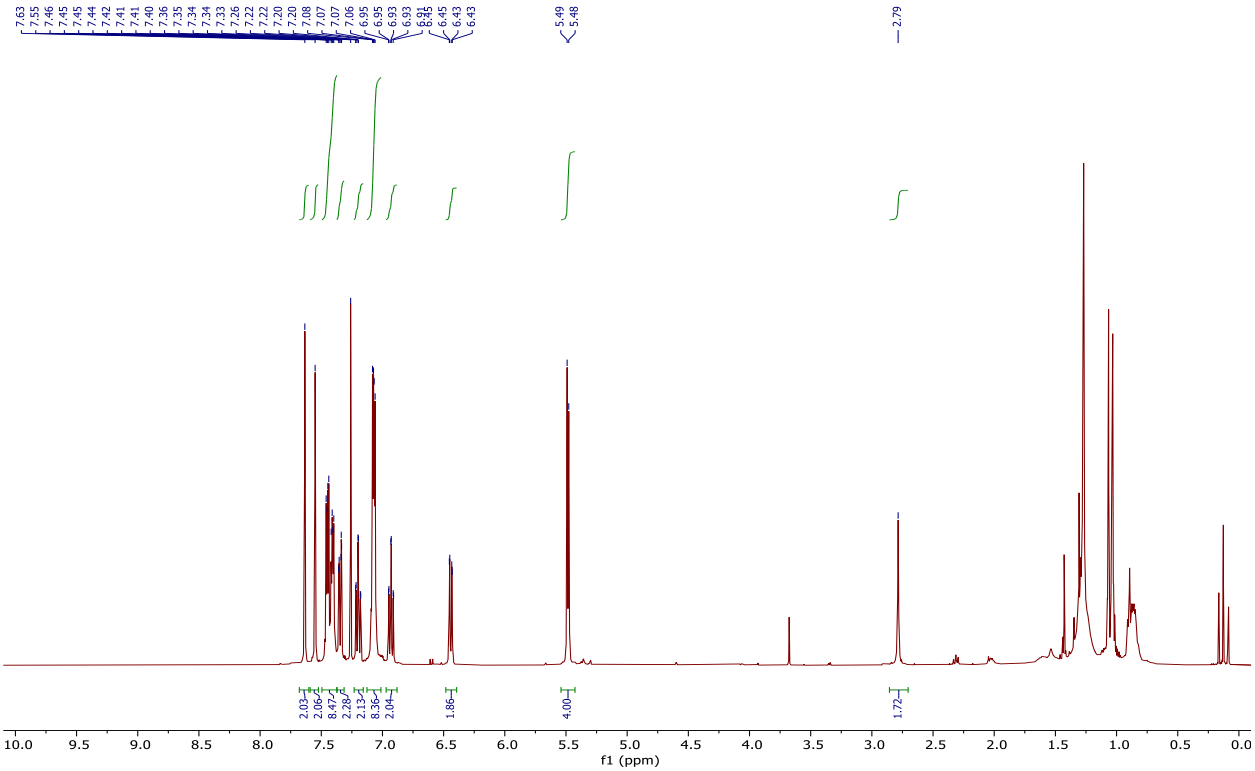

Figure S9: ^{1}H NMR of 11 (400 MHz, $CDCl_3$)

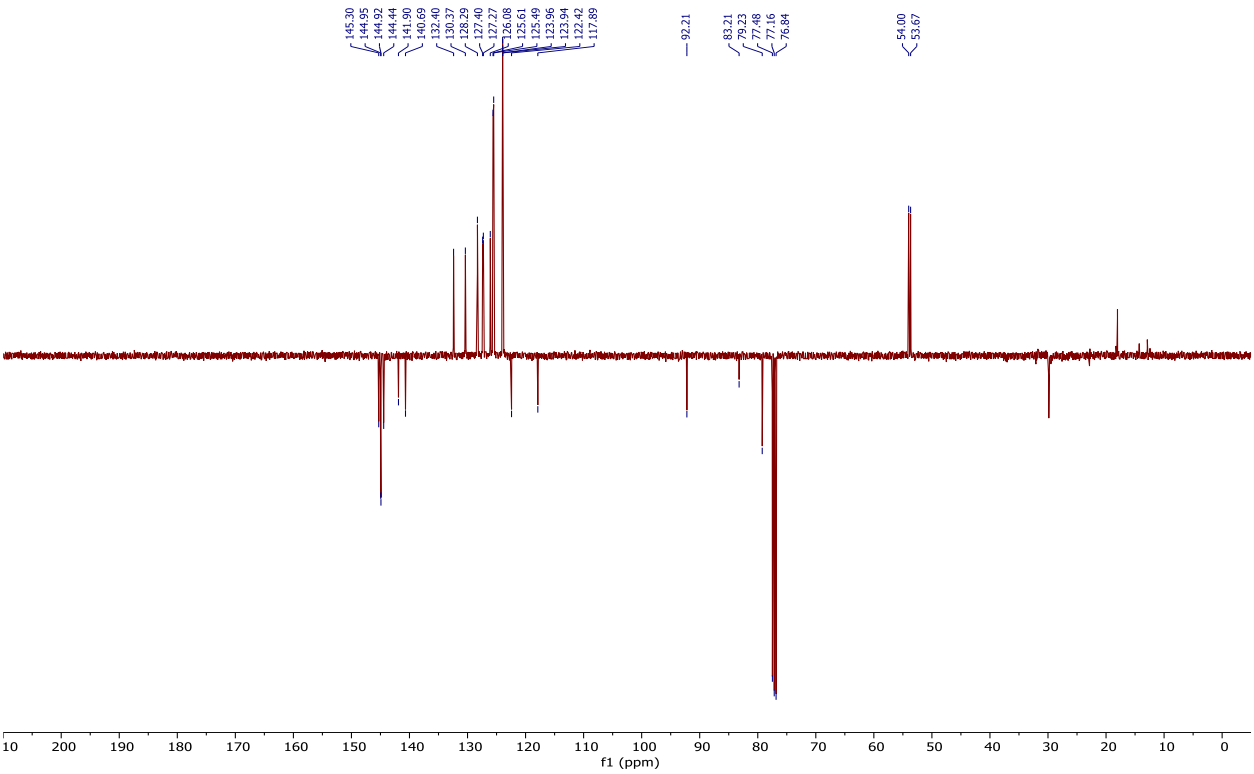

Figure S10: ^{13}C NMR of 11 (101 MHz, $CDCl_3$)

5,16,21,26-Tetrahydro-5,26:16,21-bis([1,2]benzeno)dibenzo[*f*,*j*]dinaphtho[2,3-*b*:2',3'-*n*]picene 1

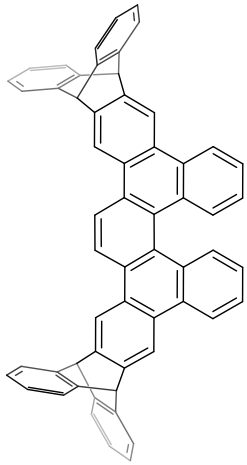

A solution of triptycenyl triyne **11** (17.5 mg, 23.9 µmol) in PhCl (1.1 mL) was degased by bubbling with nitrogen for 10 min. Then, Wilkinson's catalyst (2.2 mg, 2.4 µmol, 10 mol%) was added and the solution was degassed for further 20 min. The mixture was heated at 160 °C for 20 min in a microwave reactor. Then, volalites were evaporated under reduced pressure. The crude material was purified by column chromatography (hexane-DCM 80:20 to 50:50) to obtain ditriptyceno[5]helicene **1** (12.5 mg, 71%) as a colourless amorphous solid.

^{1}H NMR (600 MHz, $CDCl_3$): 8.61 (s, 2H, H-15), 8.60 (s, 2H, H-4), 8.56 (s, 2H, H-1), 8.45 (dd, $J_{18,19}$ = 8.4, $J_{18,20}$ = 0.9, 2H, H-18), 8.05 (dd, $J_{21,20}$ = 8.3, $J_{21,19}$ = 0.9, 2H, H-21), 7.37 – 7.45 and 7.45 – 7.51 (2 × m, 10H, H-8,11,19,25,28), 6.94 – 6.99 and 7.01 – 7.05 (2 × m, 10H, H-9,10,20,26,27), 5.66 and 5.67 (2 × s, 2 × 2H, H-6,13).

^{13}C NMR (151 MHz, $CDCl_3$): 145.00 (2 x C), 144.99, 144.97 (C-29,24,12,7), 144.37 (C-5), 144.12 (C-14), 131.04 (C-22), 130.83 (CH-21), 130.09 (C-2), 129.95 (C-17), 128.06 (C-16), 127.56 (C-23), 127.29 (C-3), 126.74 (CH-19), 125.68, 125.67, 125.60, 125.58 (CH-27,26,10,9), 124.89 (CH-20), 124.00, 123.98, 123.90, 123.89 (CH-28,25,11, 8), 123.43 (CH-19), 121.77 (CH-1), 118.58 (CH-4), 118.20 (CH-15), 54.40, 54.34 (CH-13,6).

HR MS (MALDI) m/z: ([M]$^+$) calcd for $C_{58}H_{34}$ 730.2661, found 730.2668 (Δ = 0.96 ppm).

IR ($CHCl_3$): 3072 w, 1588 w, 1468 m, 1459 vs, 1444 m, 1296 w, 1159 w, 1099 w, 1024 w, 887 m, 632 m, 626 m, 616 m, 569 m, 518 w cm^{-1}.

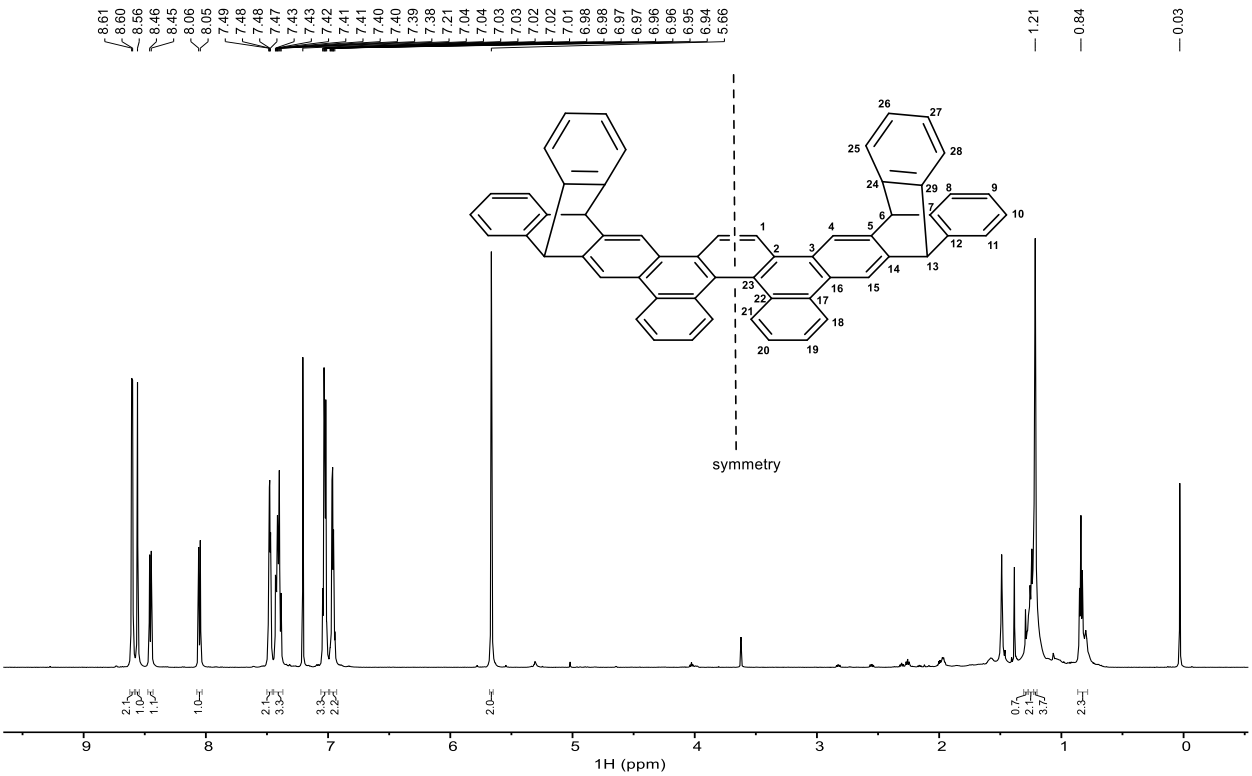

Figure S11: ^{1}H NMR of 1 (600 MHz, $CDCl_3$)

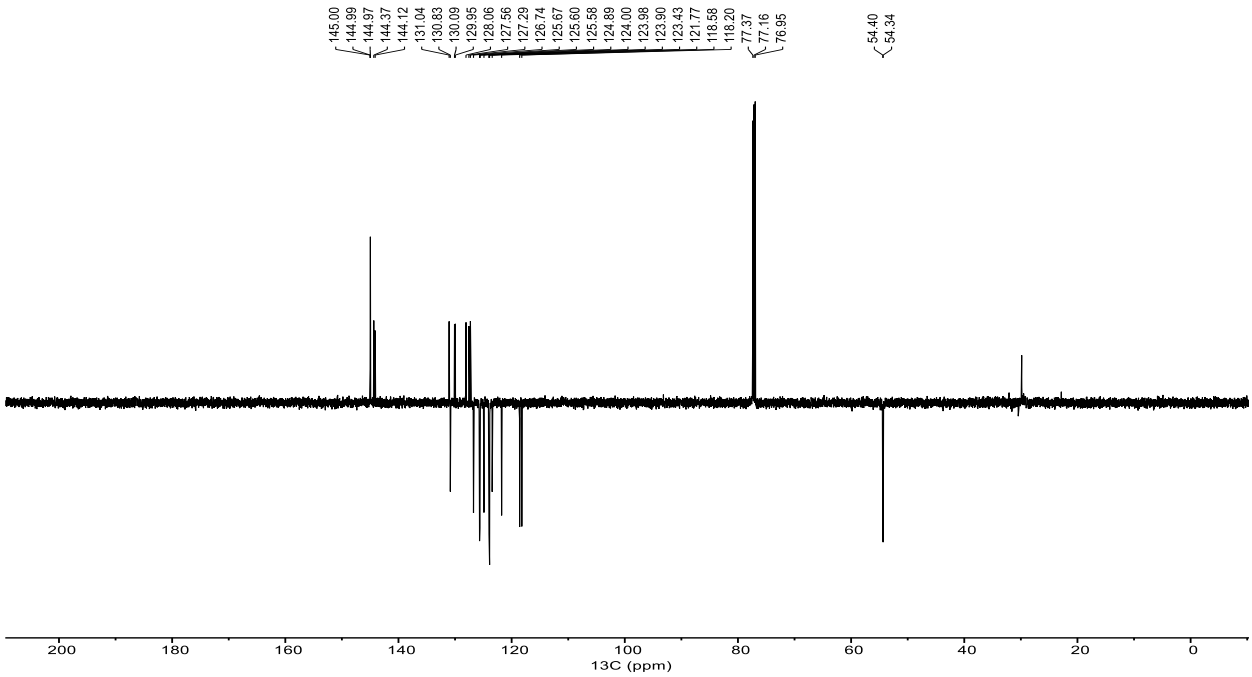

Figure S12: ^{13}C NMR of 1 (151 MHz, $CDCl_3$)

Synthesis of ditriptyceno[6]helicene 2

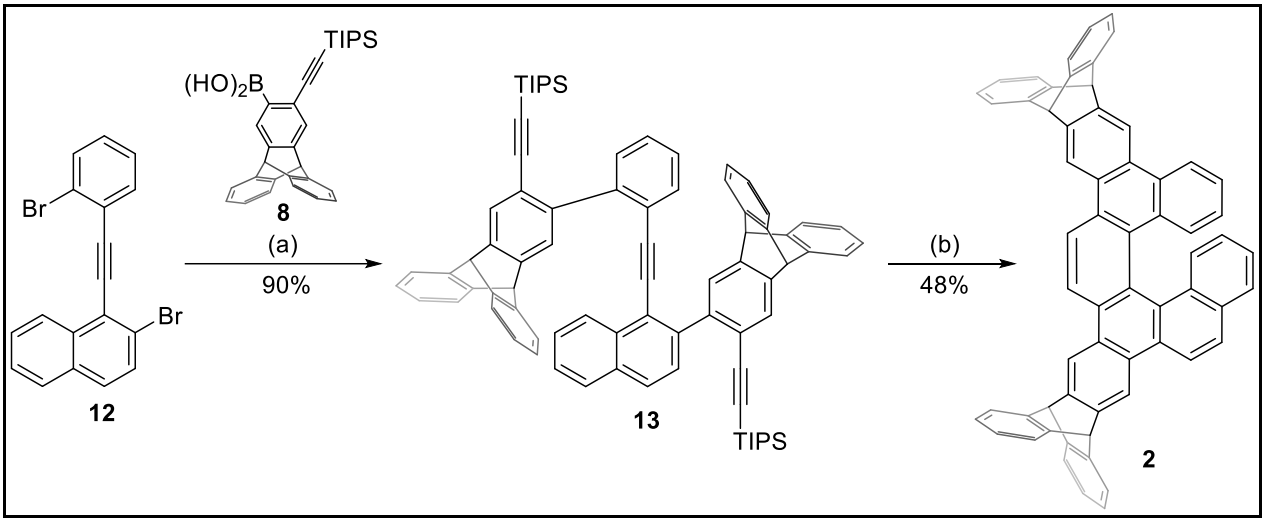

(a) Triptycenyl boronic acid **8** (2.4 equiv.), $Pd(PPh_3)_2Cl_2$ (5 mol%), Cs_2CO_3 (3.2 equiv.), toluene-EtOH-H_2O (4.3 : 4.3 : 1), 90 °C, 1.5 h, 90%; (b) *n*-TBAF in THF (1 M, 2.2 equiv.), THF, -10 °C to 0 °C, 1 h, then Wilkinson's catalyst (15 mol%), PhCl, MW, 160 °C, 30 min, 48% over two steps.

Triisopropyl((3-(2-((2-(3-((triisopropylsilyl)ethynyl)-9,10-dihydro-9,10-[1,2]benzenoanthracen-2-yl)naphthalen-1-yl)ethynyl)phenyl)-9,10-dihydro-9,10-[1,2]benzeno-anthracen-2-yl)ethynyl)silane 13

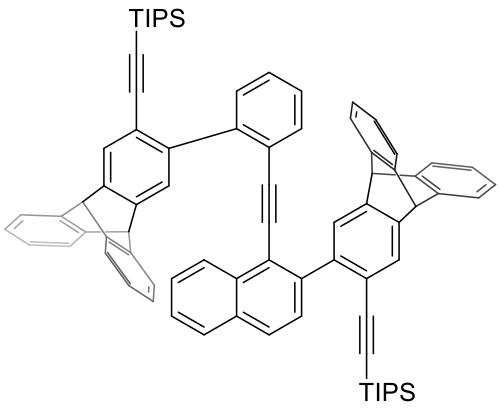

A solution of triptycenyl boronic acid **8** (290 mg, 0.61 mmol, 2.4 equiv.), 2-bromo-1-((2-bromophenyl)-ethynyl)naphthalene **12** (100 mg, 0.26 mmol), $Pd(PPh_3)_2Cl_2$ (9.1 mg, 13 µmol, 5 mol%), and Cs_2CO_3 (270 mg, 0.83 mmol, 3.2 equiv.) in a mixture of toluene-EtOH-H_2O (4.3 : 4.3 : 1, 7.6 mL) was degassed by bubbling with nitrogen for 30 min. The reaction mixture was stirred at 90 °C under nitrogen for 1.5 h. Water (5 mL) was added to quench the reaction, and the solution was extracted with DCM (3 x 10 mL). The combined organic fractions were dried over anhydrous $MgSO_4$ and evaporated under reduced pressure. The crude material was pre-adsorbed on silica gel and purified by column chromatography (hexane-DCM 95:5 to 80:20) to obtain TIPS-protected triptycenyl triyne **13** (255 mg, 90%) as a yellow amorphous solid.

^{1}H NMR (400 MHz, $CDCl_3$) δ 7.83 – 7.65 (m, 3H), 7.65 – 7.54 (m, 2H), 7.54 – 7.40 (m, 8H), 7.34 – 7.27 (m, 2H), 7.23 – 7.16 (m, 2H), 7.15 – 6.90 (m, 11H), 6.45 (d, *J* = 7.7 Hz, 1H), 5.71 (s, 1H), 5.58 (s, 1H), 5.55 (s, 1H), 5.52 (s, 1H), 5.43 (s, 1H), 0.95 (s, 42H).

^{13}C NMR (101 MHz, $CDCl_3$): δ 145.38, 145.16, 145.06, 145.02, 144.70, 144.40, 144.25, 142.80, 141.77, 141.16, 140.87, 133.18, 132.45, 132.02, 130.05, 128.16, 127.82, 127.41, 127.20, 127.15, 126.97, 126.32, 126.29, 126.17, 125.95, 125.59, 125.56, 125.45, 125.41, 125.13, 124.07, 123.90, 123.41, 120.24, 119.94, 119.70, 106.63, 106.18, 97.64, 93.23, 93.05, 90.22, 54.12, 54.06, 53.80, 53.73, 18.60, 18.58, 11.28, 11.26. Signals of four carbon atoms could not be localised due to co-resonance.

HR MS (MALDI) m/z: ([M+Na]$^+$) calcd for $C_{80}H_{76}NaSi_2$ 1115.5378, found 1115.5389 (Δ = 1.01 ppm).

IR ($CHCl_3$): 3065 w, 3020 w, 2957 s, 2941 s, 2863 s, 2149 m-w, 1616 w, 1589 w, 1564 w, 1505 w, 1491 w, 1459 vs, 1404 w, 1387 w, 1242 w, 1117 w, 1039 w, 1017 w, 996 m-w, 882 m, 820 m, 758 s, 745 vs, 677 s, 668 s cm^{-1}.

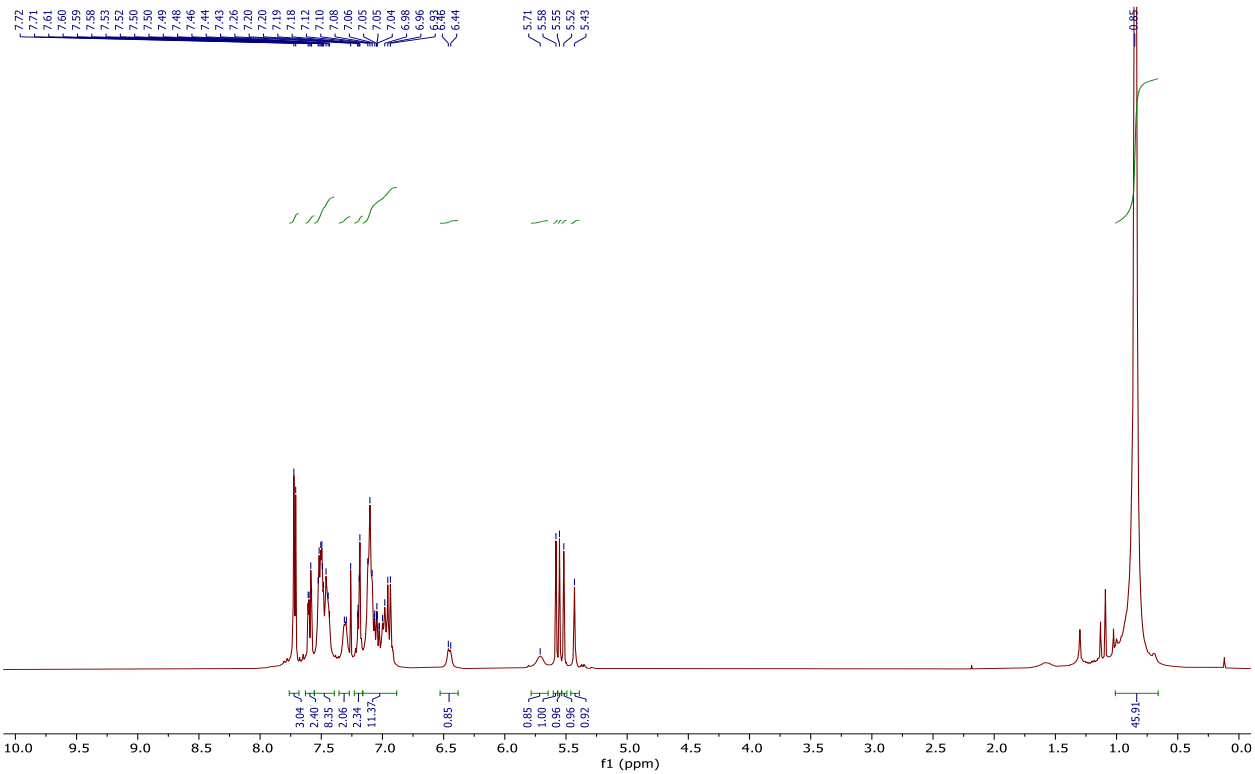

Figure S13: ^{1}H NMR of 13 (400 MHz, $CDCl_3$)

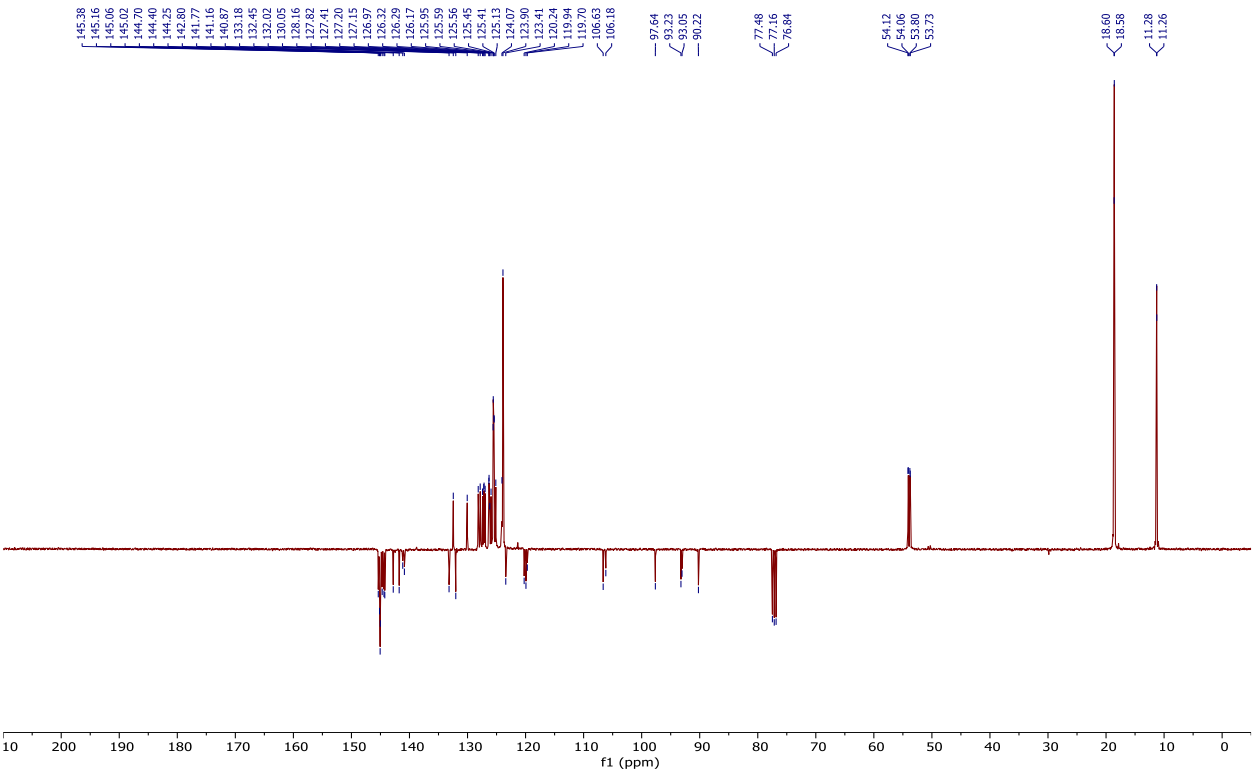

Figure S14: ^{13}C NMR of 13 (400 MHz, $CDCl_3$)

5,18,23,28-Tetrahydro-5,28:18,23-bis([1,2]benzeno)benzo[*f*]trinaphtho[2,3-*b*:1',2'-*j*:2'',3''-*n*]picene 2

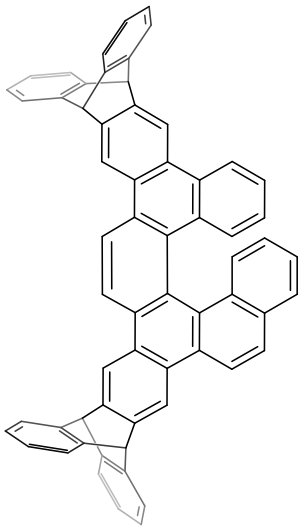

TIPS-protected triyne **13** (220 mg, 0.20 mmol) was dissolved in distilled THF (4.5 mL). An *n*-TBAF solution in THF (1 M, 0.45 mL, 0.45 mmol, 2.2 equiv.) was added dropwise at -10 °C under nitrogen. The reaction was stirred at this temperature for 30 min. Then the mixture was warmed up to 0 °C and stirred for another 30 min. After that, MeOH (0.9 mL) was added to quench the reaction and stirred at room temperature for 1 h. Then, a saturated aqueous solution of NH_4Cl (5 mL) was added and stirred for further 30 min. The solution was extracted with DCM (3 x 10 mL). The combined organic fractions were dried over anhydrous $MgSO_4$ and evaporated under reduced pressure. The crude material was pre-adsorbed on silica gel, and pre-purified by column chromatography (hexane-DCM 75:25 to 67:33) to obtain desilylated triyne (150 mg) as a yellow amorphous solid, which was used directly in the next step due to limited solubility.

Triyne from the previous step (120 mg, 0.16 mmol) in PhCl (5 mL) was degased by bubbling with nitrogen for 15 min. Then, Wilkinson's catalyst (22 mg, 24 µmol, 15 mol%) was added and degased for further 15 min. The mixture was heated at 160 °C for 30 min in a microwave reactor. Then, volatiles were evaporated and the crude material was purified by column chromatography (hexane-DCM 80:20 to 67:33) to obtain triptycenyl-[6]helicene **2** (49 mg, 48% over 2 steps) as a yellow solid.

Mp: >300 °C (hexane-DCM)

Chiral HPLC separation: *Analytical SFC*: ChiralArt Amylose-SA (150 x 3 mm, 3 µm, Alcyon YMC), 1% *i*-PrOH in DCM : CO_2 2:98 to 50:50 @ 1.5 mL/min., 35 °C, 2000 psi, t_R(+) = 5.9 min. (>99% *ee*), t_R(-) = 6.7 min. (88% *ee*); *Semipreparative HPLC*: ChiralArt Amylose-SA (250 x 20 mm, 5 µm, YMC), 50% to 70% toluene in heptane @20 mL/min.

Optical Rotation: $[\alpha]^{20}_D$ +162.4° (c 0.0570, $CHCl_3$), $[\alpha]^{20}_D$ -154.9° (c 0.0888, $CHCl_3$).

^{1}H NMR (600 MHz, $CDCl_3$): δ 8.83 (d, $J_{50,1}$ = 9.0, 1H, H-50), 8.78 (s, 3H, H-4,36,47), 8.78 (d, $J_{1,50}$ = 9.0, 1H, H-1), 8.67 (s, 1H, H-15), 8.67 (d, $J_{33,32}$ = 8.9, 1H, H-33), 8.38 (dd, $J_{18,19}$ = 8.2, $J_{18,20}$ = 1.2, 1H, H-18), 8.97 (d, $J_{32,33}$ = 8.9, 1H, H-32), 7.71 (dd, $J_{30,29}$ = 8.0, $J_{30,28}$ = 1.4, 1H, H-30), 7.48 – 7.57 (m, 8H, H-8,11,40,43,52,55,58,61), 7.36 (d, $J_{27,28}$ = 8.4, 1H, H-27), 7.18 (dd, $J_{21,20}$ = 8.3, $J_{21,19}$ = 1.3, 1H, H-21), 7.14 (ddd, $J_{19,18}$ = 8.2, $J_{19,20}$ = 6.9, $J_{19,21}$ = 1.3, 1H, H-19), 7.11 (ddd, $J_{29,30}$ = 8.0, $J_{29,28}$ = 6.7, $J_{29,27}$ = 1.1, 1H, H-29), 7.01 – 7.10 (m, 8H, H-9,10,41,42,53,54,59,60), 6.61 (ddd, $J_{28,27}$ = 8.4, $J_{28,29}$ = 6.7, $J_{28,30}$ = 1.4, 1H, H-28), 6.52 (ddd, $J_{20,21}$ = 8.3, $J_{20,19}$ = 6.9, $J_{20,18}$ = 1.2, 1H, H-20), 5.78, 5.76, 5.75, 5.74 (4 × s, 4 × 1H, H-6,13,38,45).

^{13}C NMR (151 MHz, $CDCl_3$): δ 145.13, 145.09, 144.99, 144.98, 144.97, 144.94, 144.90 (C-7,12,39,44,51,56,57,62), 144.22, 144.17, 144.15, 143.97 (C-5,14,37,46), 131.91 (C-31), 130.52 (C-49), 130.44 (C-22), 130.18 (C-26), 129.43 (C-23), 129.26 (C-17), 128.76 (C-21), 128.56 (C-2), 128.27 (C-27), 128.25 (C-32), 128.24 (C-16), 128.10 (C-35), 127.85 (C-34), 127.68, 127.67 (C-25,49), 127.45 (C-3), 127.19 (C-30), 126.14 (C-19), 125.72, 125.69, 125.67, 125.64, 125.61 (C-9,10,41,42,53,54,59,60), 125.36 (C-29), 125.14 (C-28), 124.73 (C-20), 124.06 (C-24), 124.00, 123.99, 123.97, 123.93, 123.91 (C-8,11,40,43,52,55,58,61), 122.72 (C-18), 121.76 (C-1), 121.10 (C-50), 120.87 (C-33), 118.72, 118.37, 118.27 (C-4,15,36,47), 54.41, 54.34 (C-6,13,38,45).

HR MS (MALDI) m/z: ($[M]^+$) calcd for $C_{62}H_{36}$ 780.2812, found 780.2820 (Δ = 1.03 ppm).

IR ($CHCl_3$): 3067 w, 2041 w, 3018 w, 2955 w, 2928 w, 2852 w, 1458 s, 1443 m, 1216 w, 1187 w, 1158 w, 1023 w, 881 w, 801 m, 746 vs cm^{-1}.

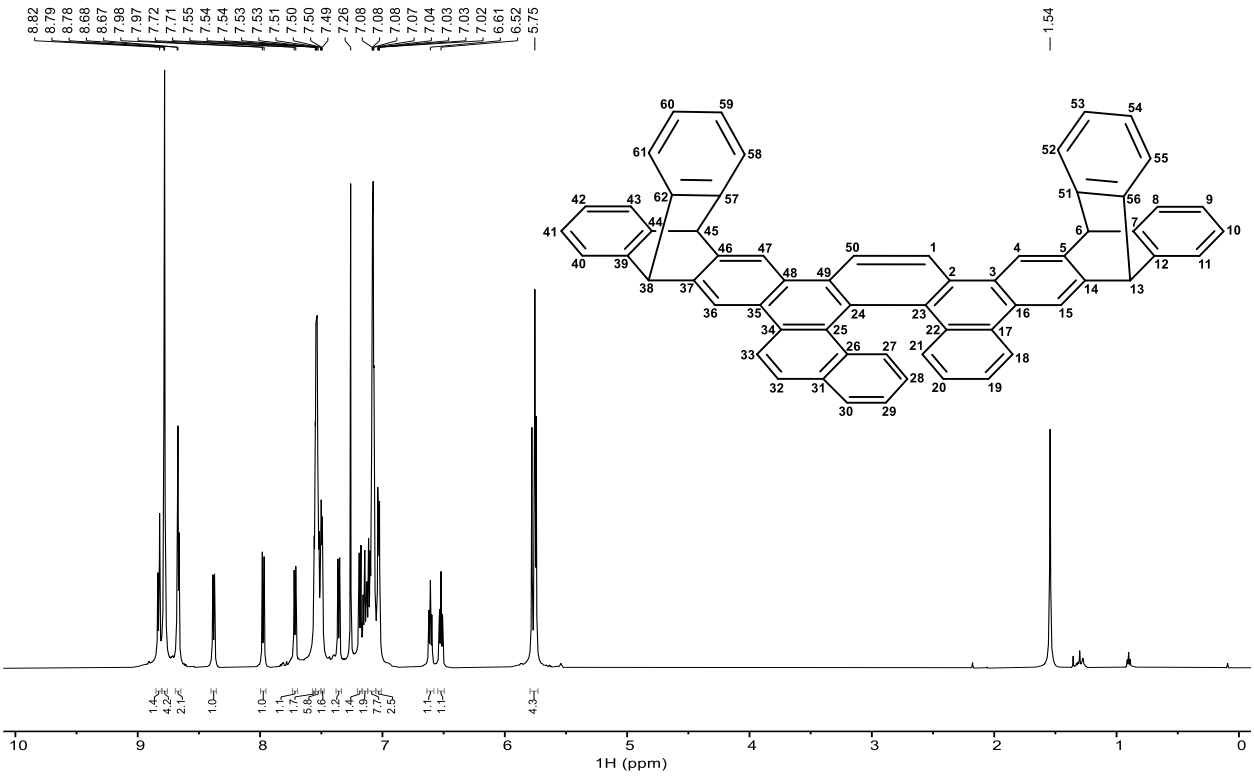

Figure S15: ^{1}H NMR of 2 (400 MHz, $CDCl_3$)

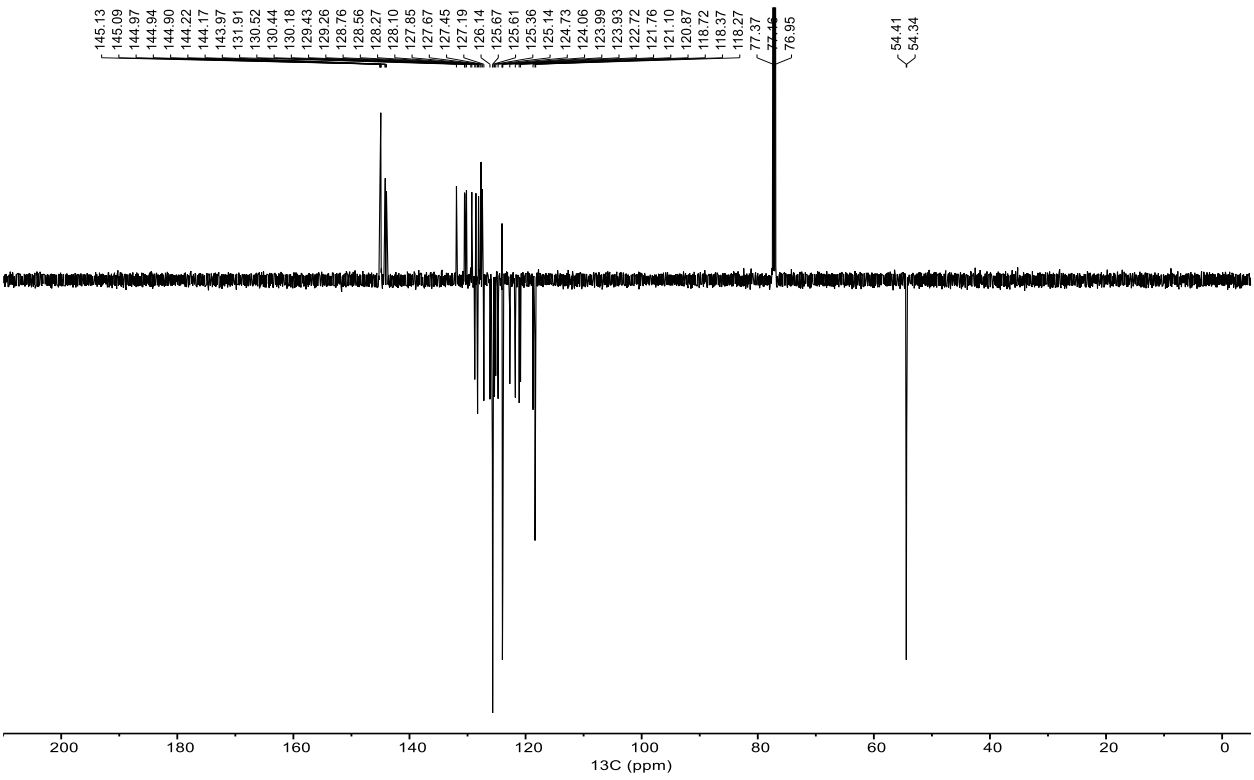

Figure S16: ^{13}C NMR of 2 (101 MHz, $CDCl_3$)

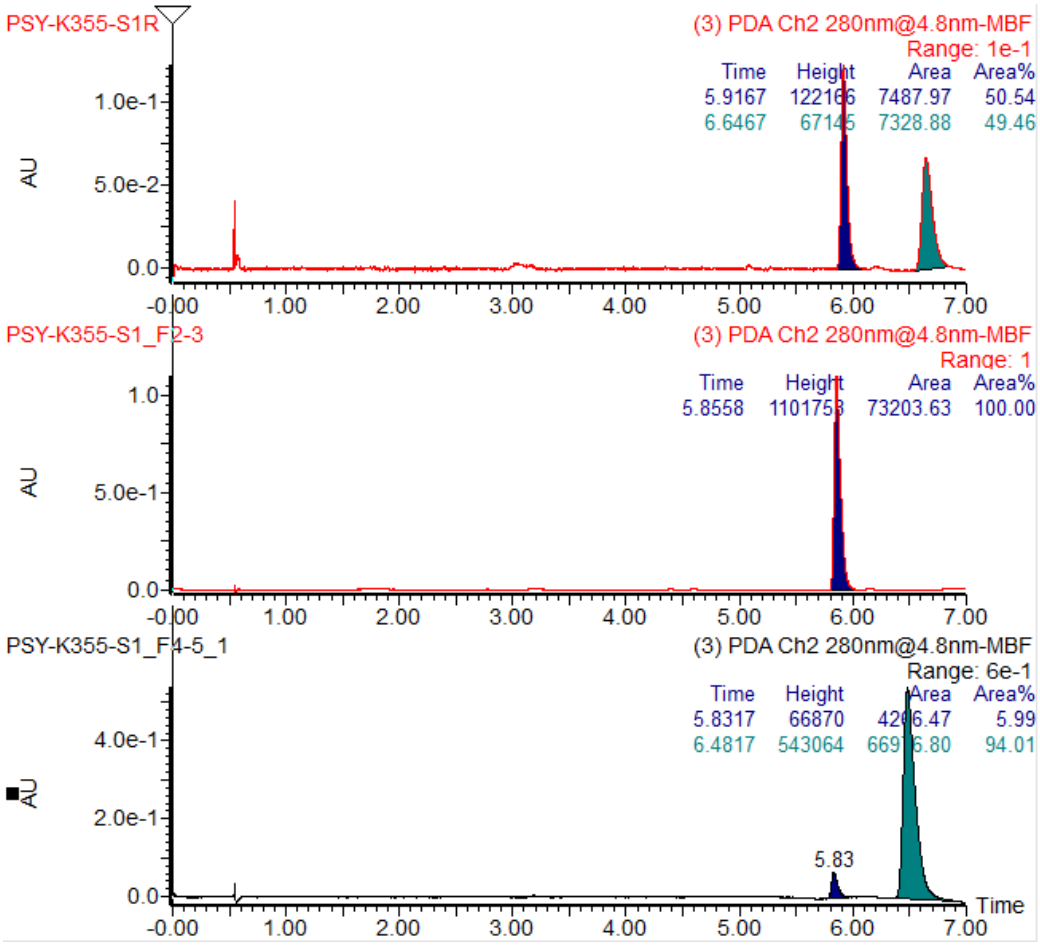

Figure S17: SFC chromatograms of *rac*-2, (+)-2 and (-)-2 (ChiralArt Amylose-SA)

Synthesis of ditriptyceno[7]helicene 3

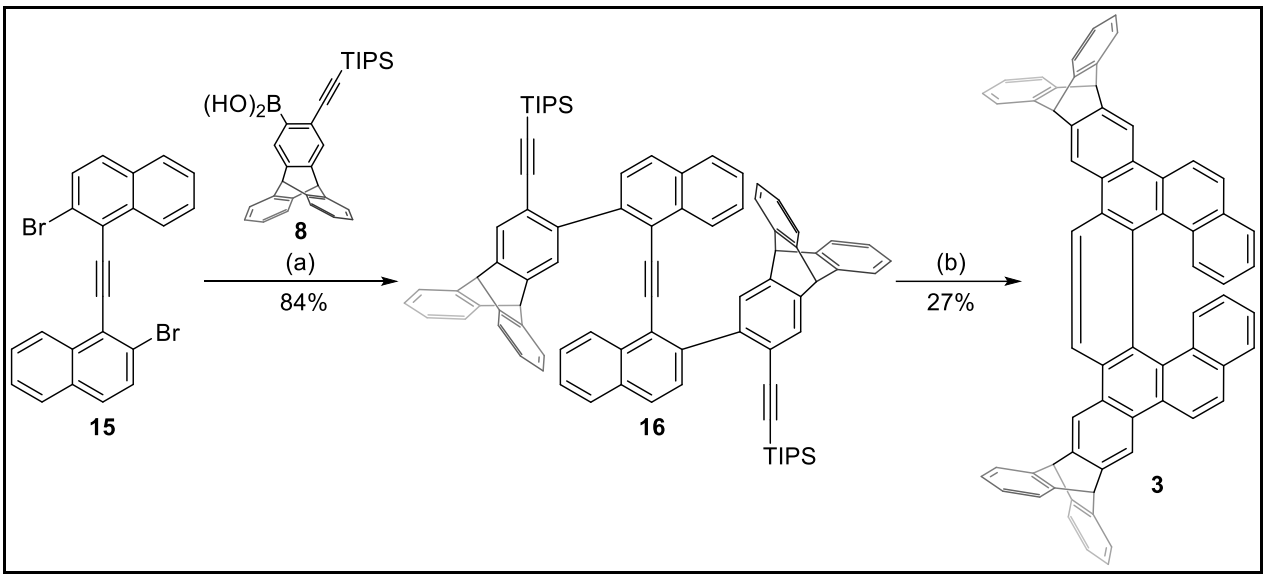

(a) Triptycenyl boronic acid **8** (2.4 equiv.), $Pd(PPh_3)_2Cl_2$ (5 mol%), Cs_2CO_3 (3.2 equiv.), toluene-EtOH-H_2O (4.3 : 4.3 : 1), 90 °C, 2 h, 84%; (b) *n*-TBAF in THF (1 M, 2.3 equiv.), THF, -10 °C to 0 °C, 1 h, then Wilkinson's catalyst (15 mol%), PhCl, mw, 160 °C, 30 min, 27% over two steps.

1-(2-(3-((Triisopropylsilyl)ethynyl)-9,10-dihydro-9,10-[1,2]benzenoanthracen-2-yl)naphthalen-1-yl)-2-(2-(3-((triisopropylsilyl)ethynyl)-9,10-dihydro-9,10-[1,2]benzenoanthracen-2-yl)naphthalen-1-yl)ethyne 16

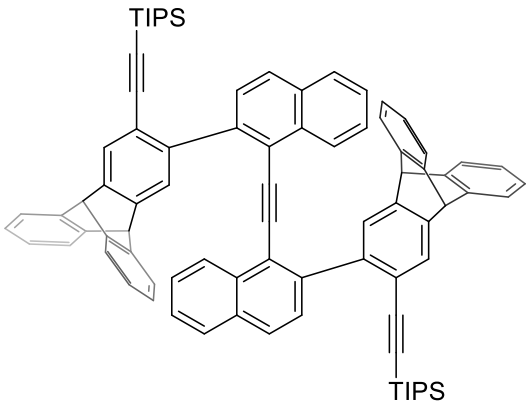

A solution of triptycenyl boronic acid **8** (516 mg, 1.08 mmol, 2.4 equiv.), 1,2-bis(2-bromonaphthalen-1-yl)ethyne **15** (200 mg, 0.459 mmol), $Pd(PPh_3)_2Cl_2$ (16.1 mg, 22.9 µmol, 5 mol%), and Cs_2CO_3 (479 mg, 1.47 mmol, 3.2 equiv.) in a mixture of toluene-EtOH-H_2O (4.3 : 4.3 : 1, 13.4 mL) was degassed by bubbling with nitrogen for 30 min. The reaction mixture was stirred at 90 °C under nitrogen for 2 h. The precipitate formed during the reaction was collected by filtration and washed with DCM (30 mL) to obtain TIPS-protected triyne **16** (439 mg, 84%) as a dull white solid.

^{1}H NMR (500 MHz, $C_2D_2Cl_4$, 80 °C) δ 7.75 (s, 2H), 7.65 (d, *J* = 8.5 Hz, 2H), 7.61 (d, *J* = 8.1 Hz, 2H), 7.59 – 7.54 (m, 6H), 7.35 (d, *J* = 7.3 Hz, 4H), 7.28 (d, *J* = 8.5 Hz, 2H), 7.15 (t, *J* = 7.4 Hz, 4H), 7.10 – 6.99 (m, 8H), 5.80 (t, *J* = 7.8 Hz, 2H), 5.62 (s, 2H), 5.46 (s, 2H), 0.68 (s, 42H).

^{13}C NMR (126 MHz, $C_2D_2Cl_4$, 80 °C) δ 145.15, 144.99, 144.93, 144.03, 142.40, 140.98, 133.04, 131.86, 127.51, 127.24, 126.59, 126.23, 126.03, 125.66, 125.35, 125.16, 124.80, 123.86, 123.73, 120.43, 120.40, 105.75, 95.39, 93.41, 53.97, 53.67, 18.12, 10.96. One CH carbon signal is missing due to co-resonance.

HR MS (MALDI) m/z: ([M+H]$^+$) calcd for $C_{84}H_{79}NaSi_2$ 1143.5715, found 1143.5724 (Δ = 0.79 ppm).

IR ($CHCl_3$): 3068 w, 3055 w, 3040 w, 3018 w, 2957 w, 2940 w, 2860 m-w, 2149 w, 1587 w, 1566 w, 1503 w, 1487 w, 1457 s, 1381 w, 1364 w, 1252 w, 1141 w, 1117 w, 1017 m-w, 996 m-w, 882 s, 865 m-w, 822 s, 750 vs, 678 s, 665 s cm^{-1}.

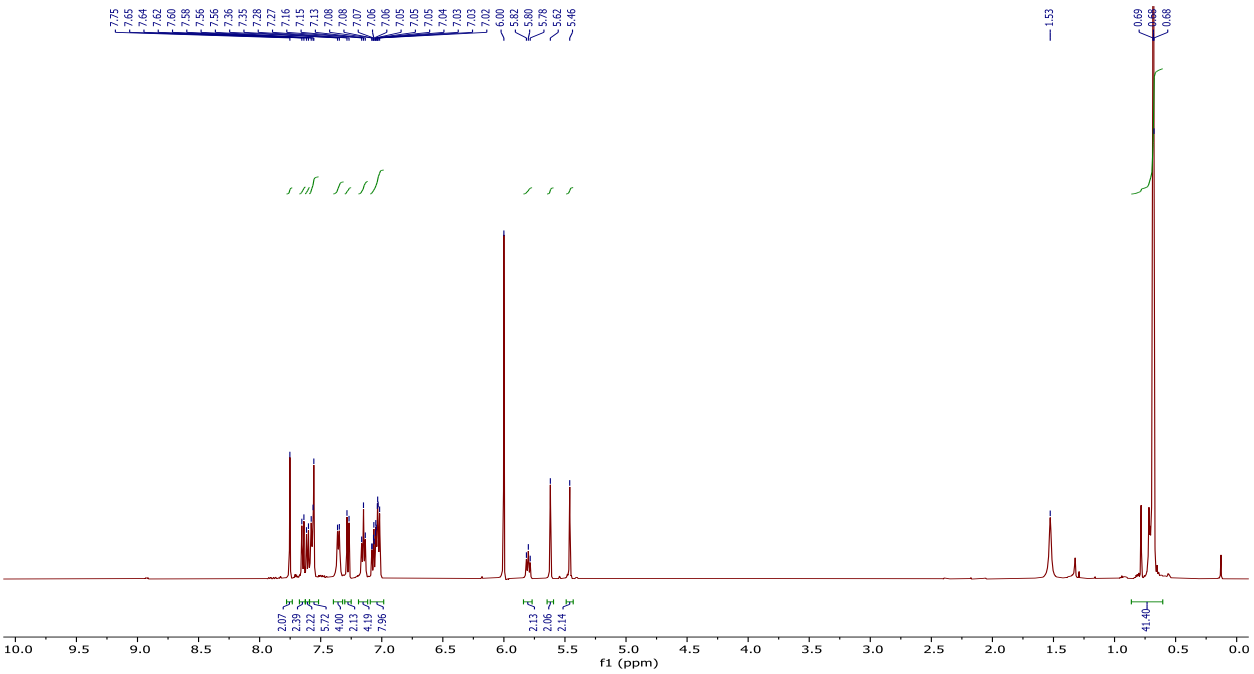

Figure S18: ^{1}H NMR of 16 (500 MHz, $C_2D_2Cl_4$, 80 °C)

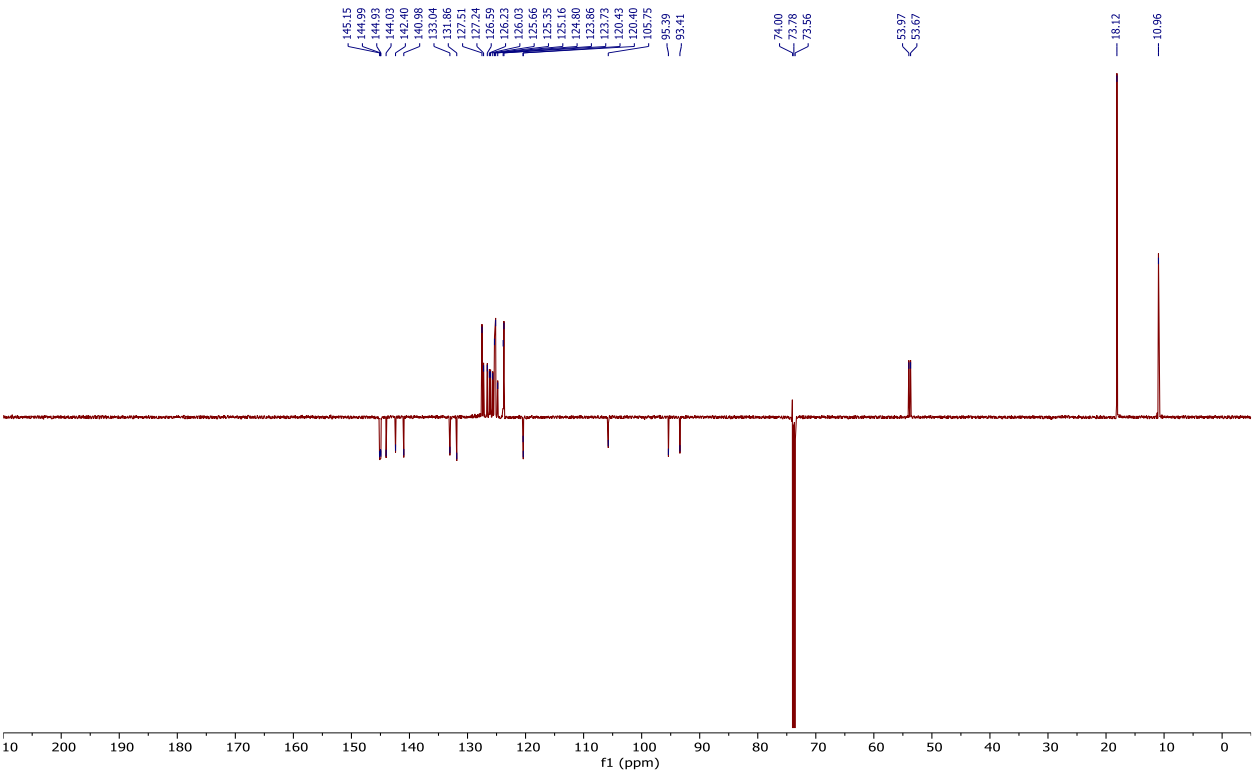

Figure S19: ^{13}C NMR of 16 (126 MHz, $C_2D_2Cl_4$, 80 °C)

5,20,25,30-Tetrahydro-5,30:20,25-bis([1,2]benzeno)tetranaphtho[2,3-*b*:2',1'-*f*:1'',2''-*j*:2''',3'''-*n*]picene 3

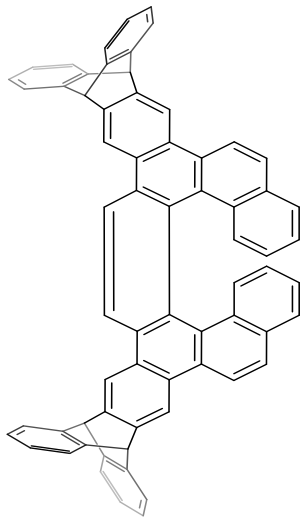

TIPS-protected triptycenyl triyne **16** (153 mg, 0.1374 mmol) was dissolved in distilled THF (3 mL). An *n*-TBAF solution in THF (1 M, 0.30 mL, 0.30 mmol, 2.2 equiv.) was added dropwise at -10 °C under nitrogen. The reaction was stirred at this temperature for 30 min. Then the mixture was warmed up to 0 °C and stirred for further 30 min. After that, MeOH (0.6 mL) was added to quench the reaction and stirred at room temperature for 1 h. The precipitate formed during the reaction was collected by filtration and washed with MeOH (10 mL) to obtain desilylated triyne (83 mg) as a dull white solid, which was used directly in the next step without purification. The crude triyne from the previous step (83 mg, 0.16 mmol) was dissolved in PhCl (3.1 mL) and degased by bubbling with nitrogen for 15 min. Then, Wilkinson's catalyst (14 mg, 15 µmol, 15 mol%) was added and degased for further 15 min. The mixture was heated at 160 °C for 30 min in a microwave reactor. Then, volalites were evaporated and the crude material was purified by column chromatography

(hexane-DCM 90:10 to 80:20) to obtain triptycenyl-[7]helicene **3** (31 mg, 27% over 2 steps) as a yellow solid.

Mp: >300 °C (hexane-DCM)

Chiral HPLC separation: *Analytical SFC*: ChiralArt Amylose-SA (150 x 3 mm, 3 µm, Alcyon YMC), CO_2 – 1% *i*-PrOH in DCM 50:50 @ 1.5 mL/min., 35 °C, 2000 psi, t_R(+) = 1.3 min. (>99% *ee*), t_R(-) = 2.1 min. (>99% *ee*); *Semipreparative HPLC*: ChiralArt Amylose-SA (250 x 20 mm, 5 µm, YMC), heptane – toluene 40:60 to 0:100 @20 mL/min.

Optical Rotation: $[\alpha]^{20}_D$ +419.6° (c 0.0347, $CHCl_3$), $[\alpha]^{20}_D$ -415.0° (c 0.0294, $CHCl_3$).

^{1}H NMR (600 MHz, THF-d_8): δ 9.09 (s, 2H, H-1), 9.02 (s, 2H, H-4), 8.87 (s, 2H, H-15), 8.55 (dd, $J_{18,19}$ = 8.6, $J_{18,24}$ = 1.0, 2H, H-18), 7.48 – 7.56 (m, 10H, H-8,11,19,29,32), 7.21 (dd, $J_{21,22}$ = 8.0, $J_{21,23}$ = 1.4, 2H, H-21), 6.98 – 7.05 (m, 8H, H-9,10,30,31), 6.80 (ddd, $J_{22,21}$ = 8.0, $J_{22,23}$ = 6.7, $J_{22,24}$ = 1.0, 2H, H-22), 6.69 (dq, $J_{24,23}$ = 8.4, $J_{24,18}$ = $J_{24,21}$ = $J_{24,22}$ = 1.0, 2H, H-24), 6.32 (ddd, $J_{23,24}$ = 8.4, $J_{23,22}$ = 6.7, $J_{23,21}$ = 1.4, 2H, H-23), 5.87 (s, 2H, H-6), 5.84 (s, 2H, H-13).

^{13}C NMR (151 MHz, THF-d_8): δ 146.41, 146.35, 146.25, 146.23 (C-7,12,28,33), 145.50, 145.46 (C-5,14), 132.29 (C-20), 130.34 (C-2,25), 129.10 (C-17), 129.03 (C-16), 128.90 (C-3), 128.38 (C-19), 126.91 (C-21), 126.85 (C-27), 126.45 (C-24), 126.14, 126.10, 126.09 (C-9,10,30,31), 125.02 (C-22), 124.91 (C-23), 124.63, 124.60, 124.59, 124.55 (C-8,11,29,32), 122.03 (C-1), 120.95 (C-18), 119.24 (C-4,15), 55.20 (C-6,13).

HR MS (MALDI) m/z: ($[M]^+$) calcd for $C_{66}H_{38}$ 830.2968, found 830.2978 (Δ = 1.16 ppm).

IR ($CHCl_3$): 3069 w, 3041 w, 3021 w, 3004 w, 2958 w, 2921 w, 2851 w, 1456 m, 1443 m, 1260 w, 1188 w, 1158 w, 1023 m-w, 882 m, 821 m-w, 800 vs, 745 vs cm^{-1}.

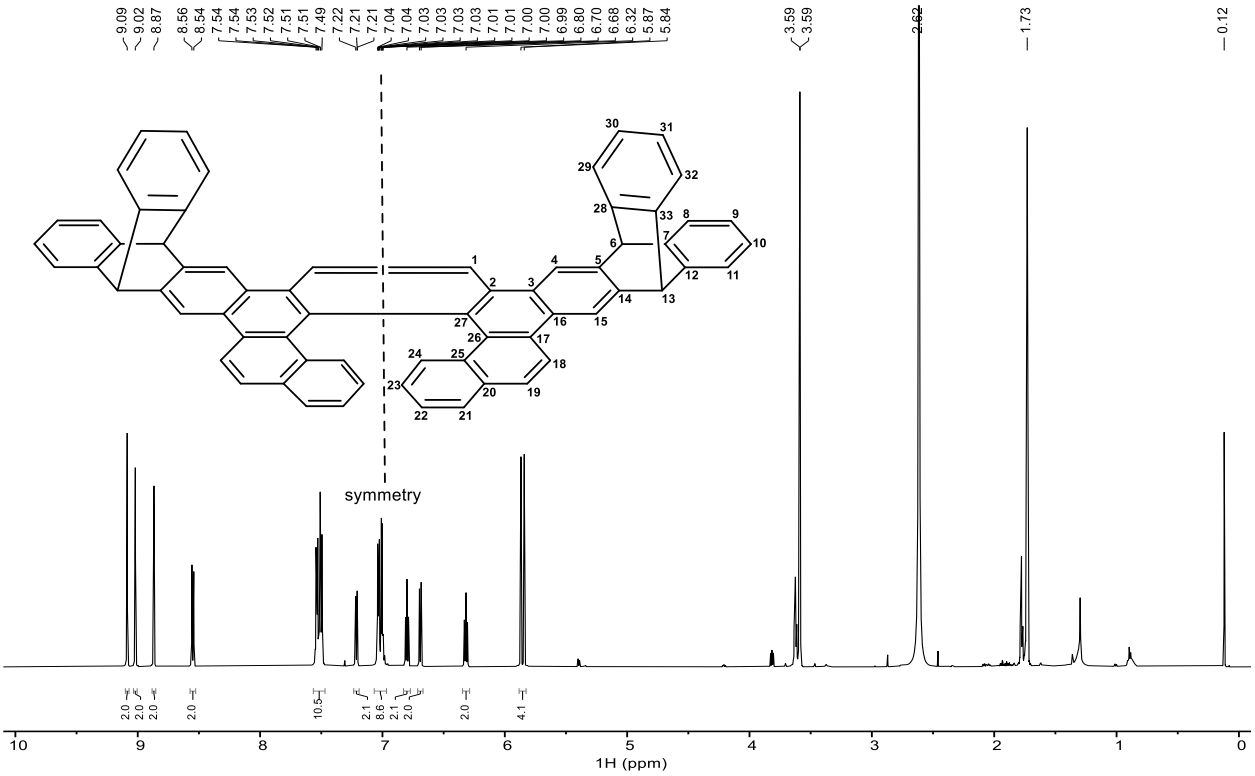

Figure S20: ^{13}C NMR of 3 (600.1 MHz, THF-d_8)

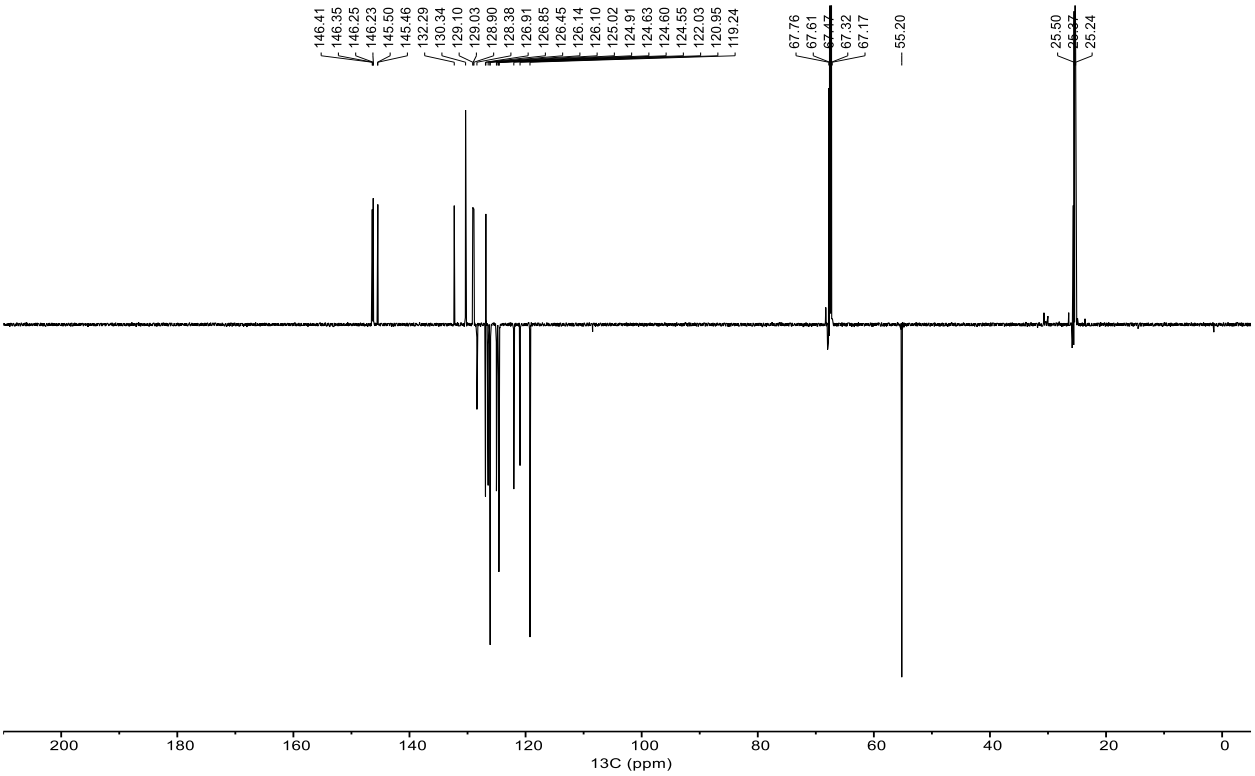

Figure S21: ^{13}C NMR of 3 (150.9 MHz, THF-d_8)

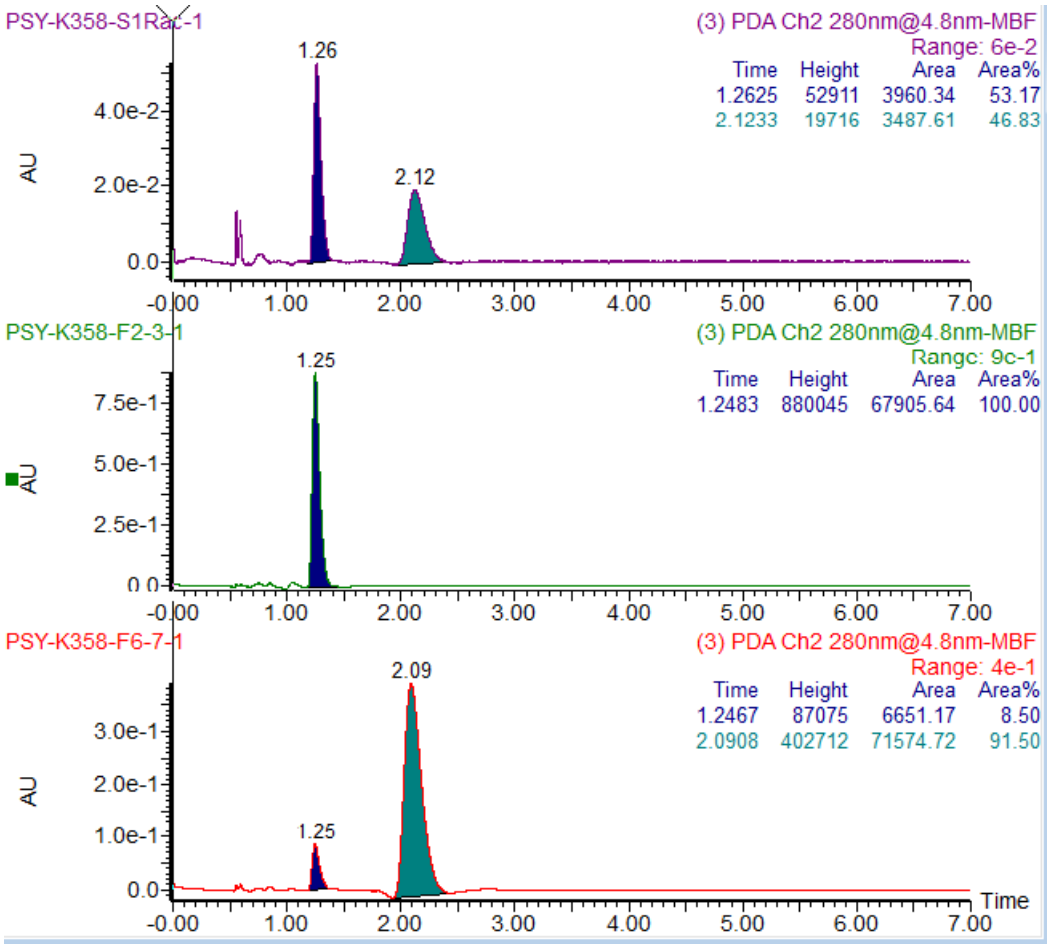

Figure S22: SFC chromatograms of *rac*-3, (+)-3 and (-)-3 (ChiralArt Amylose-SA)

X-Ray Crystallography

X-ray single crystal experiment for ditriptyceno[7]helicene **3** was performed on Bruker D8 VENTURE Kappa Duo PHOTONIII by IμS micro-focus sealed tube CuKα (λ= 1.54178 Å), equipped with Oxford Cryostream 1000 cooler. The structure was solved by direct methods (XT[5]) and refined by full matrix least squares based on F^2 (SHELXL2019[6]). The hydrogen atoms were fixed into idealised positions (riding model) and assigned temperature factors $H_{iso}(H)$ = 1.2 U_{eq}(pivot atom).

The crystals of **3** grown by slow evaporation of THF in an NMR tube exhibit a peculiar real structure. The solvating THF molecules are vastly disordered, giving to rise strong lines of diffuse scattering along c* axis. The intensity of diffuse scattering is either smooth with one dominating peak at points of reciprocal lattice or could be split into local peaks, very close to each other, depending on the treatment of the single crystal during selection of sample and adjustment on goniometer (seven crystals were tested). In addition, the diffraction pattern is even more complicated by the twinning, one twin matrix: 1 0 0; 0 -1 0; -0.50, 0 -1 suggests a pseudo-merohedral twin, the second one -1 0 0; 0 -1 0; 0.58 0 1 leads to a non-merohedral twin. The volume ratio of twin blocks was refined as 0.140 and 0.168 for first and second twin, respectively.

The real structure strongly affects the precision of the structure of the THF solvent, nevertheless, the structural parameters of the helical molecule were determined reliably.

Crystal data for **3**: $C_{66}H_{38}\cdot3(C_4H_8O)$, M_r = 1047.27; Monoclinic, $P2_1/n$ (No 14), a = 8.0567 (6) Å, b = 15.9953 (7) Å, c = 44.136 (2) Å, β = 93.047 (4)°, V = 5679.7 (6) Å^3, Z = 4, D_x = 1.225 Mgm^{-3}, temperature of sample 100(2) K, colourless plate of dimensions 0.33 × 0.15 × 0.09 mm, multi-scan absorption correction (μ = 0.56 mm^{-1}), T_{min} = 0.837, T_{max} = 0.951; a total of 54188 measured reflections (θ_{max}= 72.3°), from which 11099 were unique (R_{int} = 0.040) and 10887 observed according to the $I > 2\sigma(I)$ criterion. The refinement converged ($\Delta/\sigma_{max} <$ 0.001) to R = 0.134 for observed reflections and w$R(F^2)$ = 0.326, GOF = 1.19 for 720 parameters and all 54188 reflections (due to the twinning, the diffractions were not merged during refinement). The final difference map displayed no peaks of chemical significance ($\Delta\rho_{max}$ = 0.87, $\Delta\rho_{min}$ -0.65 e.Å^{-3}).

X-ray crystallographic data have been deposited with the Cambridge Crystallographic Data Centre under deposition numbers CCDC 2492687. They can be obtained free of charge from the Centre via its website (https://www.ccdc.cam.ac.uk/structures/).

[5] SHELXT: G. M. Sheldrick, *Acta Cryst.* 2015, **A71**, 3-8.
[6] SHELXT: G. M. Sheldrick, *Acta Cryst.* 2015, **C71**, 3-8.

DFT calculations

All calculations were performed using the Gaussian 16 software package.[7]

Geometries of all studied structures were optimised by DFT (B3LYP[8]/cc-pVTZ[9]/GD3[10]). In all cases, vibrational analysis confirmed absence of imaginary frequencies (or presence of one imaginary frequency in case of transition states). RRHO approximation was used for calculation of free energies (298 K, 1 atm). The QST3 method[11] was used for location of transition states. Cartesian coordinates (xyz files) for the final geometries (ground states of (*M*)-**1**, (*M*)-**2**, (*M*)-**3**, and first and second excited states of (*M*)-**3**), and for racemization transition state geometries are part of the supplementary information.

For the simulation of ECD and absorption spectra, optimised geometries from previous step were used. Absence of imaginary frequencies was always confirmed by vibrational analysis. The ECD and absorption spectral traces were simulated by extracting vertical excitations from TD-DFT calculations of 145 lowest-lying singlet states at the CAM-B3LYP[12]/cc-pVTZ/GD3 level of theory and applying gaussian broadening (0.4 eV) and red shift (25 nm) to the resulting line spectra (Energy vs Oscillator or Rotational strength). A full list of TD-DFT absorption and ECD transitions is given below.

(*M*)-**2**: Wavelength, Osc. Strength, Rot. Strength: 344.898, 0.0017, -0.1842; 336.767, 0.0721, -31.7894; 310.169, 0.8401, -77.2192; 302.584, 0.0299, 11.3843; 291.254, 0.0166, -94.6385; 286.609, 0.5778, 150.2262; 283.801, 0.0356, -24.9632; 273.828, 0.2138, 27.07; 268.73, 0.09, 67.8978; 263.841, 1.4055, -578.3037; 260.964, 0.1003, -63.6583; 257.677, 0.23, 57.5638; 253.256, 0.0806, -52.4814; 246.783, 0.0556, -85.7037; 245.488, 0.1621, 201.1959; 242.099, 0.2412, 178.2522; 237.74, 0.0309, -14.4364; 237.617, 0.0388, 6.0737; 234.72, 0.1422, 260.4146; 233.897, 0.1983, 136.3039; 231.538, 0.0159, -9.8357; 231.016, 0.0122, 15.5643; 230.115, 0.0008, -1.8701; 228.854, 0.2101, 287.6002; 228.214, 0.0013, -12.7262;

---

[7] Gaussian 16, Revision C.01, M. J. Frisch, G. W. Trucks, H. B. Schlegel, G. E. Scuseria, M. A. Robb, J. R. Cheeseman, G. Scalmani, V. Barone, G. A. Petersson, H. Nakatsuji, X. Li, M. Caricato, A. V. Marenich, J. Bloino, B. G. Janesko, R. Gomperts, B. Mennucci, H. P. Hratchian, J. V. Ortiz, A. F. Izmaylov, J. L. Sonnenberg, D. Williams-Young, F. Ding, F. Lipparini, F. Egidi, J. Goings, B. Peng, A. Petrone, T. Henderson, D. Ranasinghe, V. G. Zakrzewski, J. Gao, N. Rega, G. Zheng, W. Liang, M. Hada, M. Ehara, K. Toyota, R. Fukuda, J. Hasegawa, M. Ishida, T. Nakajima, Y. Honda, O. Kitao, H. Nakai, T. Vreven, K. Throssell, J. A. Montgomery, Jr., J. E. Peralta, F. Ogliaro, M. J. Bearpark, J. J. Heyd, E. N. Brothers, K. N. Kudin, V. N. Staroverov, T. A. Keith, R. Kobayashi, J. Normand, K. Raghavachari, A. P. Rendell, J. C. Burant, S. S. Iyengar, J. Tomasi, M. Cossi, J. M. Millam, M. Klene, C. Adamo, R. Cammi, J. W. Ochterski, R. L. Martin, K. Morokuma, O. Farkas, J. B. Foresman, D. J. Fox, Gaussian, Inc., Wallingford CT, 2016.

[8] A. D. Becke, *J. Chem. Phys*. 1993, **98**, 5648-5652.

[9] R. A. Kendall, T. H. Dunning Jr., R. J. Harrison, *J. Chem. Phys.* 1992, **96**, 6796.

[10] S. Grimme, J. Antony, S. Ehrlich, H. Krieg, *J. Chem. Phys.* 2010, **132**, 154104.

[11] C. Peng, H. B. Schlegel, *Israel J. Chem.*, 1993, **33**, 449-54.

[12] T. Yanai, D. Tew, N. Handy, *Chem. Phys. Lett.* 2004, **393**, 51-57.

227.907, 0.0016, 15.6723; 225.63, 0.0685, 72.1755; 223.6, 0.0658, -11.8848; 223.033, 0.0376, 10.2132; 221.297, 0.0721, -100.7524; 218.956, 0.041, -40.99; 216.725, 0.0064, 12.2267; 215.71, 0.0284, 27.0732; 213.843, 0.0032, -15.8956; 213.067, 0.0149, -14.8518; 210.406, 0.3592, -30.5633; 209.954, 0.0398, -12.2524; 206.936, 0.0044, -0.9728; 206.874, 0.0068, -1.2328; 206.063, 0.0384, -14.4982; 205.827, 0.0051, 16.1198; 205.098, 0.0005, 3.5655; 204.621, 0.0072, -3.4226; 203.8, 0.0698, 44.3304; 203.646, 0.0534, -33.7827; 203.336, 0.0799, 3.5301; 202.813, 0.0422, -27.4343; 201.915, 0.0652, -57.1758; 201.803, 0.0085, 24.5798; 201.6, 0.0012, -2.76; 200.641, 0.0072, 10.2518; 200.274, 0.0559, 51.0848; 199.344, 0.0012, 1.7473; 198.925, 0.0033, -12.381; 198.403, 0.0017, -7.4418; 197.587, 0.0585, -71.3063; 197.423, 0.0229, 79.2585; 197.131, 0.0389, -163.3874; 197.016, 0.0982, -52.0196; 196.457, 0.0192, -17.147; 195.991, 0.0113, -66.1915; 195.886, 0.0312, 6.3019; 195.032, 0.0505, -55.0259; 194.469, 0.0883, -45.319; 194.414, 0.0237, -55.7459; 194.064, 0.0112, -31.2602; 193.819, 0.0288, -40.9642; 193.785, 0.0179, 34.5713; 193.338, 0.0241, 6.4652; 192.683, 0.0174, -9.9381; 192.423, 0.0362, -6.9883; 191.596, 0.0393, 27.6714; 191.038, 0.009, -1.0595; 190.853, 0.1114, -33.8011; 190.238, 0.0289, -19.7248; 189.653, 0.0982, 59.7624; 189.086, 0.0096, -12.2488; 188.968, 0.0296, 53.9685; 188.767, 0.2321, 199.5923; 188.46, 0.218, -782.5819; 188.131, 0.9269, 572.9362; 187.718, 0.0613, -74.8429; 187.275, 0.0193, 48.5262; 186.568, 0.1249, -116.6941; 186.265, 0.0815, 223.5067; 186.025, 0.0672, 20.6302; 185.863, 0.0312, 58.0774; 185.652, 0.0421, -58.2829; 184.813, 0.0146, 44.61; 184.791, 0.0705, -121.811; 184.643, 0.0164, -92.0592; 184.516, 0.0149, 26.5713; 183.854, 0.0188, -37.003; 183.628, 0.0091, 39.0869; 183.37, 0.0036, 16.719; 182.918, 0.0139, 14.5997; 182.891, 0.0052, 21.0116; 182.748, 0.0074, -16.6584; 182.552, 0.0303, 37.1159; 182.163, 0.0029, -19.7152; 182.003, 0.0002, 6.6136; 181.574, 0.0064, -23.0444; 181.486, 0.0035, -10.9895; 181.252, 0.0568, -26.4217; 181.001, 0.0147, 29.5867; 180.761, 0.0139, -12.2346; 180.374, 0.0517, 103.9585; 180.055, 0.0288, 5.3974; 179.739, 0.0322, 13.0257; 179.471, 0.0457, -17.1778; 179.209, 0.0155, -0.1394; 178.93, 0.0092, -24.0814; 178.888, 0.0021, -23.5455; 178.654, 0.1265, 80.6106; 178.404, 0.1383, -29.6529; 178.194, 0.0126, 29.9544; 178.02, 0.0852, 23.4127; 177.877, 0.035, -35.4774; 177.566, 0.0322, 71.0465; 177.181, 0.0323, -1.7693; 177.024, 0.003, -5.6565; 176.728, 0.0329, -200.547; 176.547, 0.0755, 30.3423; 176.229, 0.0219, 32.8626; 176.028, 0.013, -71.0818; 175.349, 0.117, 27.59; 175.279, 0.1239, 50.5044; 175.22, 0.0425, -167.8044; 175.049, 0.0222, -91.5257; 174.748, 0.0418, 63.9439; 174.215, 0.0662, 87.0449; 174.166, 0.0034, -37.7401; 174.083, 0.0055, -7.3488; 173.742, 0.0107, 38.4942; 173.579, 0.0603, -25.6759; 173.44, 0.0894, 48.4895; 173.372, 0.0788, 18.546; 173.082, 0.0669, 78.9775; 172.942, 0.019, -12.6191; 172.619, 0.0599, -15.7987; 172.372, 0.0934, -176.1688; 172.319, 0.0501, 39.3077; 172.264, 0.0095, -17.431; 172.009, 0.099, 50.6438; 171.737, 0.0585, -18.3617.

(*M*)-**3**: Wavelength, Osc. Strength, Rot. Strength: 354.341, 0.0007, 0.6612; 348.055, 0.1058, -72.8907; 323.938, 0.2447, -311.5005; 318.365, 0.0043, 2.2068; 314.13, 0.0018, -9.2556; 297.046, 0.0368, 48.2441; 291.803, 0.3458, 305.0299; 289.236, 0.9938, 65.4204; 283.684, 0.0139, 20.7151; 283.01, 0.249, -51.7602; 272.05, 0.1478, 120.1466; 270.849, 0.5323, -372.546; 265.053, 0.6513, -273.3134; 262.89, 0.6599, 754.1911; 255.996, 0.0487, -16.5913; 250.868, 0.0067, 64.3438; 244.337, 0.1461, -107.8711; 244.289, 0.0361, 111.814; 241.934, 0.112, 314.9925; 240.591, 0.3496, -105.6922; 237.695, 0.0004, -22.8044; 237.681, 0.0673, 28.4935; 236.48, 0.0353, 12.9981; 233.901, 0.1121, 53.184; 231.495, 0.0159, -8.1367; 231.456, 0.0216, 82.8573; 230.133, 0.0053, -5.8365; 228.113, 0, 4.841; 228.113, 0.0138, -138.0365; 227.907, 0.0891, 52.8358; 226.902, 0.0077, -15.4558; 226.091, 0.1748, 61.3612; 225.704, 0.0631, -214.0303; 224.47, 0.0074, -61.9785; 223.193, 0.017, -16.9534; 222.05, 0.0046, 21.9629; 221.578, 0.0339, -93.0285; 218.485, 0.1653, -75.7446; 218.416, 0.0016, -4.605; 217.245, 0.0165, -33.5396; 216.577, 0.0289, -48.4229; 214.843, 0.0346, -12.4596; 210.499, 0.0009, 0.2415; 209.358, 0.0002, -0.1718; 209.203, 0.0842, 31.1612; 207.755, 0.0117, 2.6642; 207.473, 0.007, -5.9766; 207.379, 0.0001, 5.2043; 207.376, 0.0111, 10.2153; 206.385, 0.0006, -0.2014; 205.36, 0.0005, 0.7587; 205.356, 0.0015, 7.183; 205.129, 0.0344, -17.703; 204.045, 0.0019, 5.9796; 203.787, 0.0013, -62.8711; 203.773, 0.1502, 10.8377; 203.069, 0, -0.1112; 202.456, 0.078, -410.3743; 202.254, 0.0006, 12.1365; 202.208, 0.0198, -21.6824; 202.014, 0.0106, -9.7528; 200.81, 0.0626, -9.4937; 200.339, 0.018, -7.101; 199.578, 0.0005, -3.9967; 199.466, 0.0017, 0.4669; 198.922, 0.0029, -2.4289; 197.827, 0.0368, -248.261; 197.76, 0.0153, 74.8377; 197.348, 0.0163, -100.3563; 197.081, 0.1329, 219.683; 196.859, 0.0006, 38.8641; 195.966, 0.3441, -421.285; 195.703, 0.0048, -45.2491; 195.324, 0.0855, 130.9718; 194.891, 0.0011, 27.0161; 194.864, 0.0542, 56.2437; 194.299, 0.0142, -70.4252; 194.192, 0.0157, -69.5588; 194.171, 0.0046, -17.8386; 193.655, 0.0264, 91.6466; 193.124, 0, -0.1006; 192.905, 0.0379, 38.3887; 191.833, 0.0376, 22.2477; 191.315, 0.0231, 26.2832; 191.215, 0.029, -121.1315; 190.715, 0, 0.5061; 190.706, 0.0042, -5.7365; 190.53, 0.0313, 95.8131; 190.501, 0.0031, 18.4913; 189.737, 0.0816, -22.0812; 189.19, 0.0166, 284.0095; 189.179, 0.0851, 47.8304; 188.787, 0.0142, -445.4921; 188.704, 0.8261, 235.6107; 188.174, 0.0165, -395.8521; 187.9, 0.739, 67.2033; 187.792, 0.0064, 149.3001; 187.145, 0.0021, 41.3403; 187.086, 0.0023, 5.0571; 186.959, 0.0352, -0.2006; 186.31, 0.0599, 21.7331; 185.986, 0.0191, 131.4156; 185.975, 0.0297, 132.3802; 185.535, 0.0459, -237.5883; 185.062, 0.0281, -14.0707; 184.72, 0.0963, 108.1485; 184.643, 0.0127, 14.9723; 184.363, 0.0003, 5.0497; 183.974, 0.0054, -11.2105; 183.928, 0.0294, -13.5723; 183.819, 0.0114, 39.5745; 183.674, 0.0134, 28.3886; 183.113, 0.0053, -2.2697; 182.851, 0.0065, -7.4054; 182.45, 0.0118, 39.6626; 181.989, 0.0079, 38.9788; 181.912, 0.0269, -108.6293; 181.611, 0.0562, 75.9127; 181.499, 0.0251, -94.774; 181.099, 0.0197, 35.0468; 181.07, 0.0542, 37.7107; 181.004, 0.0176, 41.0718; 180.787, 0.0446, 42.5722; 180.695, 0.029, -38.1653; 180.624, 0.1242, -11.2072; 180.448, 0.0007, -0.7031; 180.364, 0.0064,

18.6261; 180.261, 0.0279, 22.4756; 179.874, 0.0066, 28.0825; 179.77, 0.0136, 4.2112; 179.281, 0.023, -13.1623; 178.515, 0.2995, 66.6905; 178.474, 0.1071, 7.0425; 178.325, 0.0165, 3.818; 178.271, 0.0099, 49.2829; 177.887, 0.0097, -29.114; 177.869, 0.0314, -72.6291; 177.849, 0.1137, 68.7726; 177.841, 0.0243, 69.4049; 177.681, 0.0402, 19.9143; 177.678, 0.1406, 74.055; 177.274, 0.0304, 43.8107; 177.175, 0.0134, -22.7898; 177.135, 0.0463, -30.7772; 177.064, 0.0123, -165.6911.

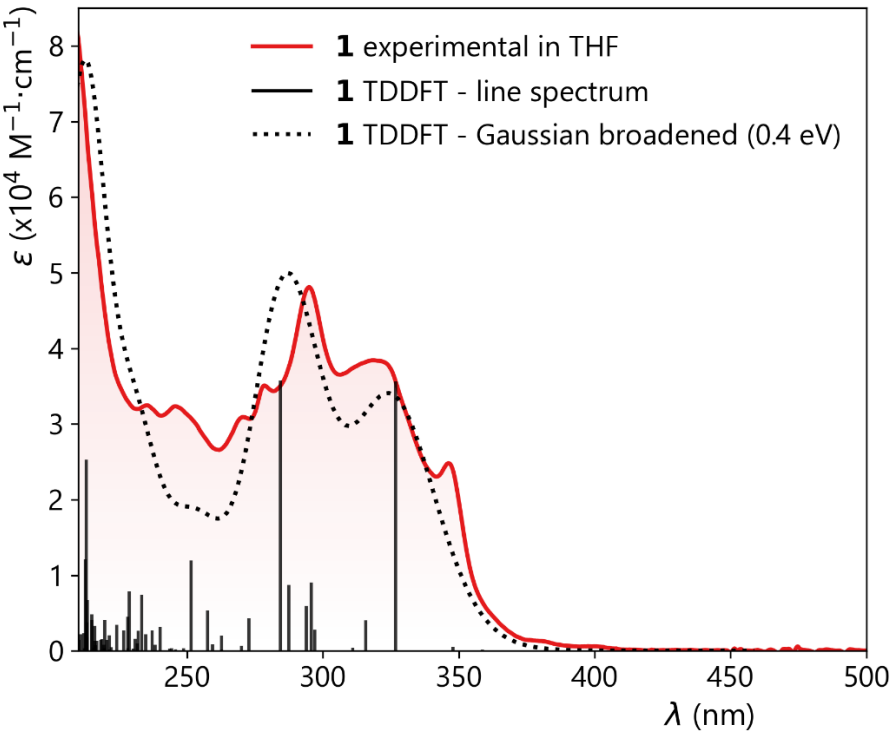

Figure S23: Overlay of experimental (in THF) and TDDFT-simulated (in vacuum) absorption spectrum of 1

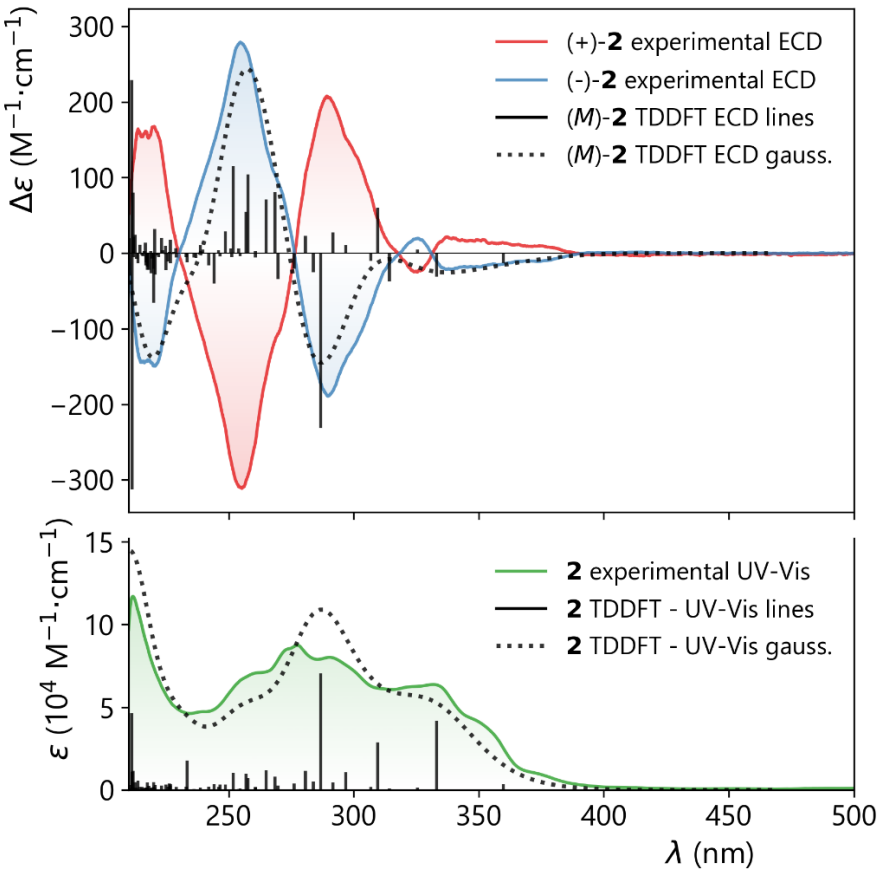

Figure S24: Overlay of experimental (in THF) and TDDFT-simulated (in vacuum) absorption and ECD spectra of 2

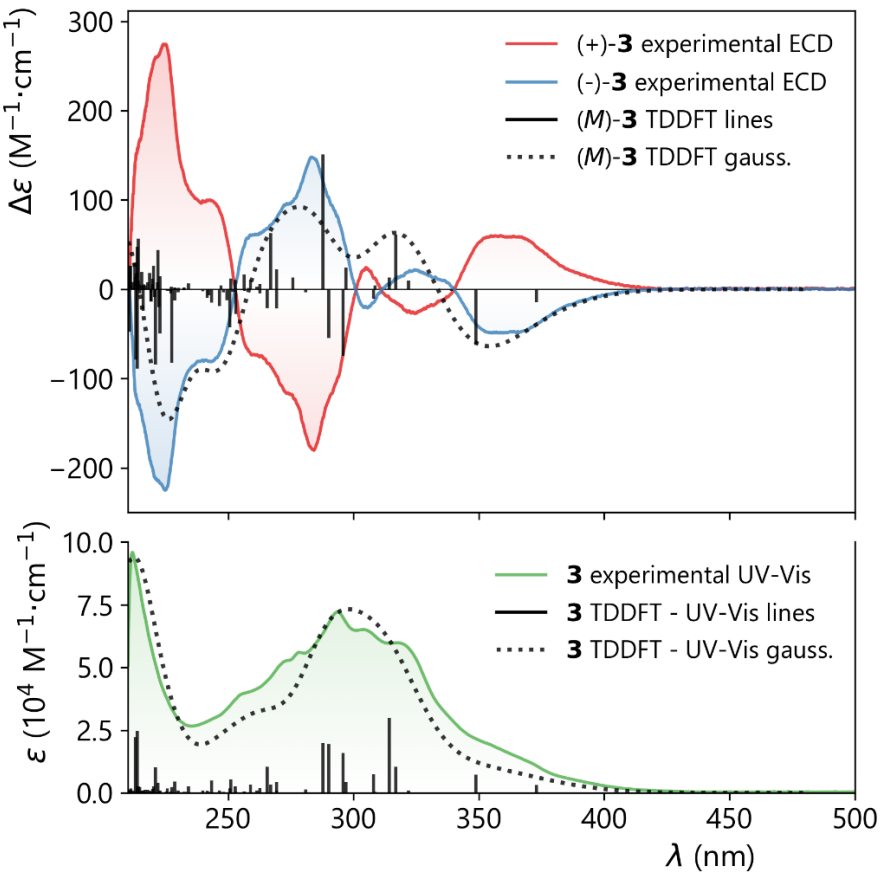

Figure S25: Overlay of experimental (in THF) and TDDFT-simulated (in vacuum) absorption and ECD spectra of 3

Helicity assignment

The absolute configuration of the resolved helicenes **2** and **3** was assigned based on reasonable agreement between the experimental (measured in THF at 10^{-4} M concentration) and simulated (TDDFT) spectra of electronic circular dichroism (ECD). As can be seen from Figures S24 and S25 above, the fast-eluting dextrorotatory enantiomers are of ***P*** configuration, while the slow-eluting laevorotatory ones are of ***M*** helicity.

Emission properties

The geometries of the first 5 excited singlet states of (*M*)-**3** were optimized at the CAM-B3LYP /cc-pVTZ/GD3 TD-DFT level (NStates=6). Resulting emissive states from S_1-S_5 are summarised in Table S1.

Table S1: Lowest lying excited states of (*M*)-3 calculated by TD-DFT[a]

State	Emission Wavelength (nm)	Oscillator Strength	Rotational Strength
S1	489.08	0.1130	-122.0137
S2	386.55	0.0011	1.1990
S3	333.58	0.0030	-13.3179
S4	328.72	0.0238	6.5443
S5	306.70	0.9039	163.9610

[a]Calculated by TD-DFT (CAM-B3LYP/cc-pVTZ/GD3).

Electronic properties of ditriptycenohelicenes 1–3 and parent [5]-, [6]- and [7]helicenes 18–20

Table S2: Electronic properties of ditriptycenohelicenes 1–3 and parent [5]-, [6]- and [7]helicene 18–20

Helicene	First excited state HOMO-LUMO gap (eV)[a]	Optical HOMO-LUMO gap (eV)[b]
1	3.72	3.18
[5]Helicene **18**	3.70	3.44
2	3.59	3.02
[6]Helicene **19**	3.34	3.33
3	3.50	2.95
[7]Helicene **20**	3.17	3.12

[a]Calculated by TD-DFT (CAM-B3LYP/cc-pVTZ/GD3), singlet state (E_{SOMO2}-E_{SOMO1}). [b]Based on the onset of the longest-wavelength band in the UV-Vis spectrum.

Racemisation barriers of ditriptycenohelicenes 1–3

In the case of the pentahelicene-based compound **1**, due to low thermal stability of the enantiomers, the racemisation barrier was experimentally measured by the dynamic HPLC method.[13] The racemate was resolved by analytical HPLC using Chiralpak IC (250 x 4.6 mm ID, 5 µm, DAICEL) column and 30% DCM in heptane @ 0.5 mL/min at 30 and 40 °C, under which conditions racemisation takes place on the column. Although no clear plateau was observed, the chromatogram could still be processed using the DCXplorer software,[14] giving the free energy of activation of 25.2 kcal/mol and 25.6 kcal/mol at 30 and 40 °C, respectively, which is in good agreement with the value calculated by DFT (26.6 kcal/mol at 25 °C).

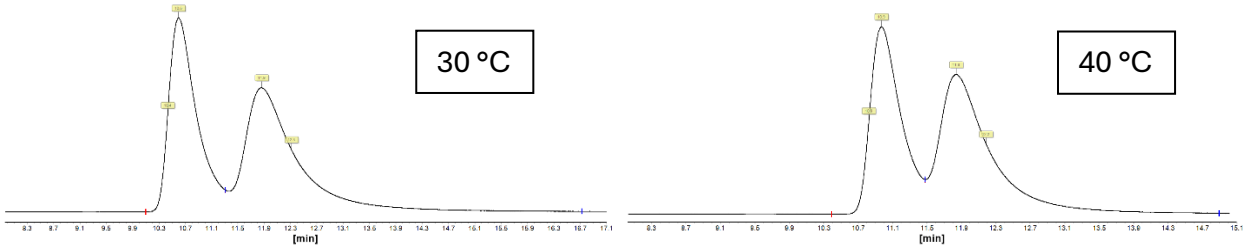

Figure S26: On-column racemisation of 1

Table S3: Critical parameters from dynamic HPLC experiments with 1

T (°C)	t_R^A (min)	t_R^B (min)	hw^A (s)	hw^B (s)	h^P (%)	k_1 (x10^{-6} s^{-1})	$\Delta G^{\ddagger}$ (kcalmol^{-1})
30	10.61	11.88	19.8	54.2	11.36	3.91	**25.2**
40	10.95	11.81	17.8	41.6	18.32	7.89	**25.6**

t_R = retention time, hw = peak half-width, h^P = relative height of the plateau

Racemisation of the ditriptyceno[6]helicene derivative **2** was carried out at 200 °C in hexadecane (1 mg in 1 mL). Every 10 minutes, aliquots (50 µL) were taken out and quickly cooled to room temperature before being analysed by SFC. The barrier was then calculated from Eyring equation for first order reversible reaction (equilibrium ratio of enantiomers is 50:50) using a rate constant k_{obs} (=$2k_1$) from the slope of the plot of -ln(fractional *ee*) *vs*. time.

[13] O. Trapp, *Chirality* 2006, **18**, 489-497.
[14] O. Trapp, *J. Chromatogr. B*, 2008, **875**, 42-47.

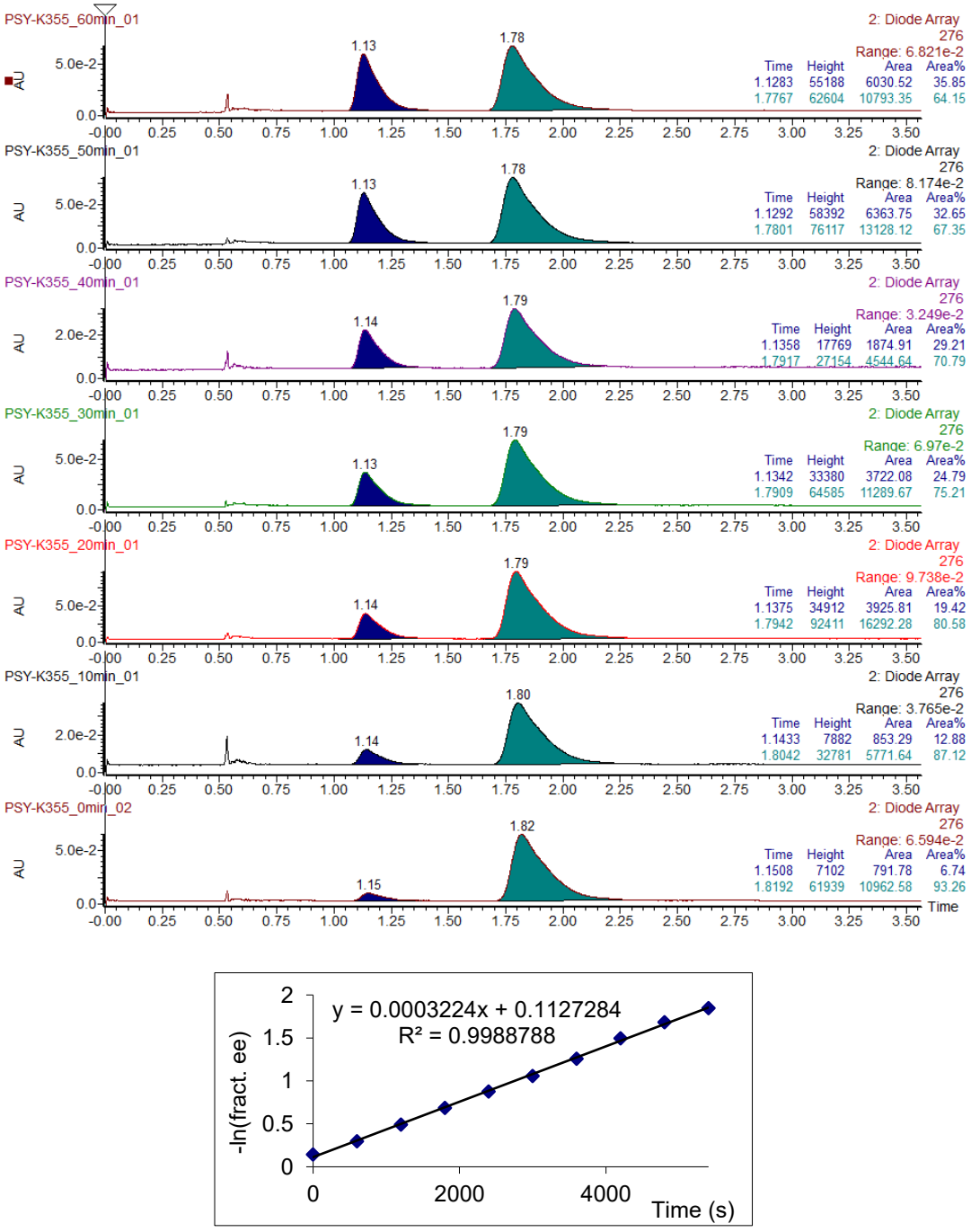

Figure S27: Racemisation kinetics of 2 (in hexadecane at 200 °C)

Using the procedure above for compound **3** did not allow us to measure the racemisation barrier, as the compound did not observably racemise at 200 °C within 8 hour time, which is our technical limit. This suggests $k_{obs} < 10^{-6}$ s^{-1} and the corresponding $\Delta G^{\ddagger}$ >41 kcalmol^{-1}, which is in line with the racemisation barriers of [7]helicene derivatives.

Table S4: Barriers to racemisation of ditriptyceno[n]helicenes 1, 2, 3 (n = 5–7) and parent [n]helicenes 18–20 (n = 5–7)

Helicene	Experimental[a] (kcal mol^{-1})	Calculated[b] (kcal mol^{-1})
1	25.2	26.7
[5]Helicene **18**	24.1[c]	
2	36.3	35.7
[6]Helicene **19**	36.2[d]	
3	>41	41.1
[7]Helicene **20**	41.7[d]	

[a]Measured in *n*-heptane-CH_2Cl_2 (3:7) with 0.1 % isopropanol at 30 °C (**1**) or in hexadecane at 200 °C (**2**), estimated for **3**. [b]Calculated by DFT B3LYP/cc-pVTZ/GD3, corrected to 25 °C (RRHO method). [c]In isooctane, corrected to 20 °C.[15] [d]In naphthalene, corrected to 27 °C.[16]

[15] C. Goedicke and H. Stegemeyer, *Tetrahedron Lett*, 1970, 937–940.
[16] R. H. Martin and M.-J. Marchant, *Tetrahedron Lett.*, 1972, **13**, 3707–3708.

Circularly polarised luminescence

CPL spectra of *P* and *M* enantiomers of ditriptyceno[n]helicenes (n=6,7) **2** and **3** show mirror-image traces with moderate g_{lum} factors of ±2.3 x 10^{-3} (at 425 nm) and ±0.9 x 10^{-3} (at 430 nm), respectively, when measured in THF at 10^{-5} M concentration. Interestingly, although the heptahelicene based compound **3** features only one emission band, its CPL spectrum is split into two bands with opposite polarity. Similar behaviour is also observed in toluene solutions. The sign of the CPL emission (the higher-energy band in case of **3**) is in both cases opposite to the sign of optical rotation and the sign of the lowest-energy cotton band in ECD, *i.e.* negative for the fast-eluting (+)-(*P*)-**2**/**3** and positive for the slow-eluting (-)-(*M*)-**2**/**3**.

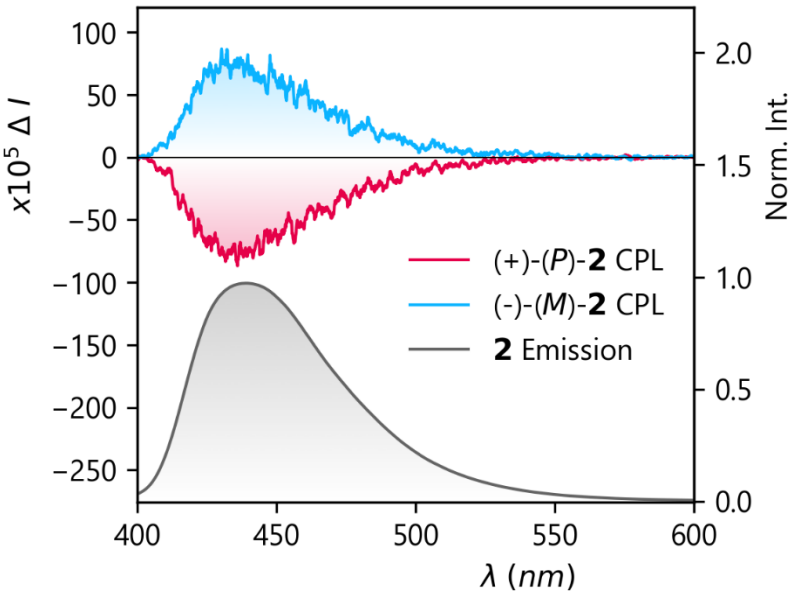

Figure S28: CPL spectra of 2 (10^{-5} M in THF)

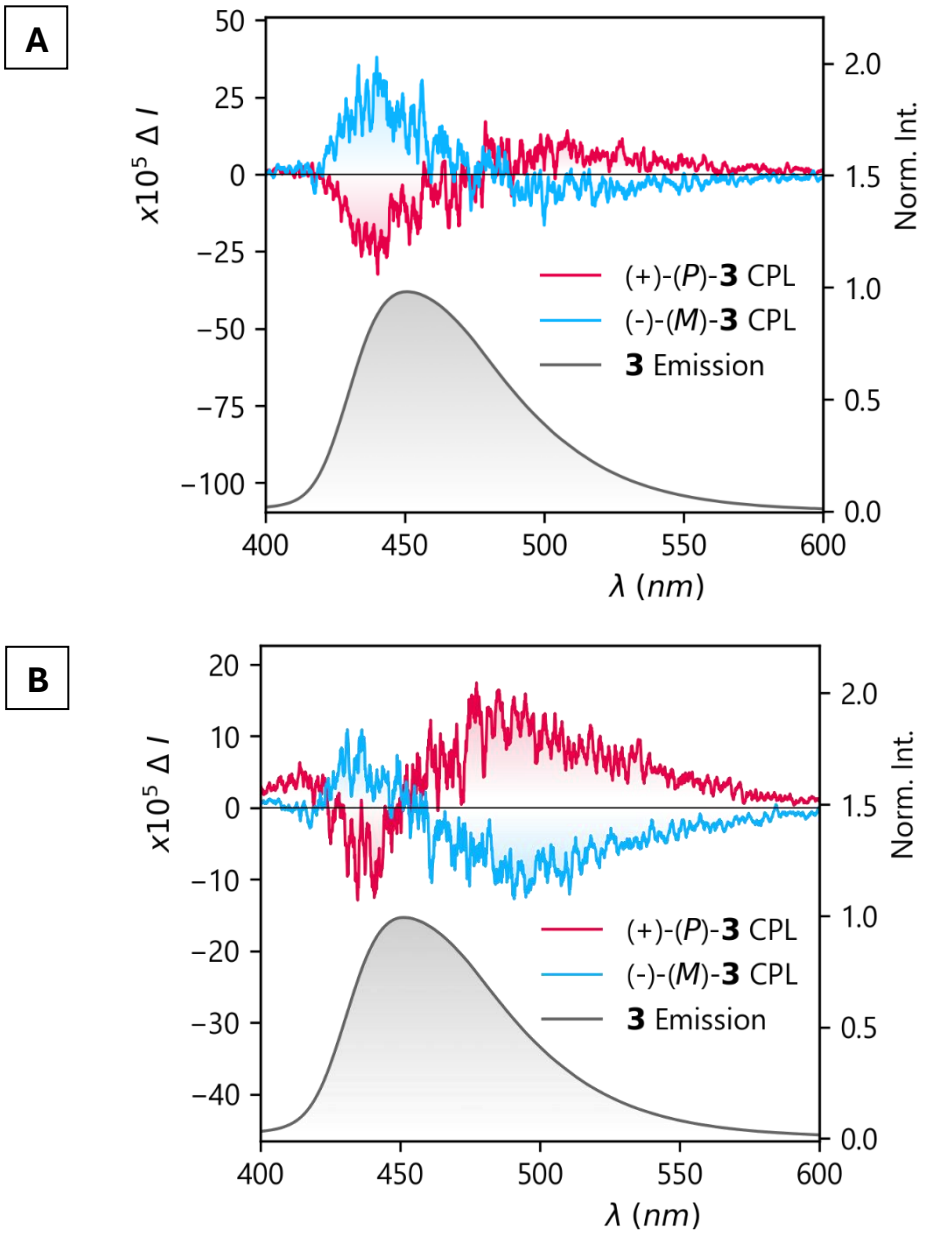

Figure S29: CPL spectra of 3 (**A**: 10^{-5} M in THF, **B**: 10^{-5} M in toluene)

Table S5: Calculated[a] chiroptical properties of emissive states of ditriptycenoheptahelicene 3 in vacuum.

State	λ_{em} (nm)	f^{b}	R^{c} (10^{-40} cgs)	μ^{d} (au)	m^{e} (au)	Θ^{f} (^{o})	g_{lum}	τ^{g} (ns)	Symmetry
S_1	489	0.113	-122	1.34	1.954	106[h]	-0.0041	20	B
S_2	386	0.001	+1.2	0.12	0.014	0[i]	0.0054	2000	A

[a]TD-DFT CAM-B3LYP/cc-pVTZ/GD3. [b]Oscillator strength. [c]Rotatory strength. [d]Electric transition dipole moment. [e]Magnetic transition dipole moment. [f]Angle between transition dipole moments. [g]Calculated lifetime of fluorescence. [h]In a plane perpendicular to the C_2 axis. [i]Colinear in C_2 symmetry axis.

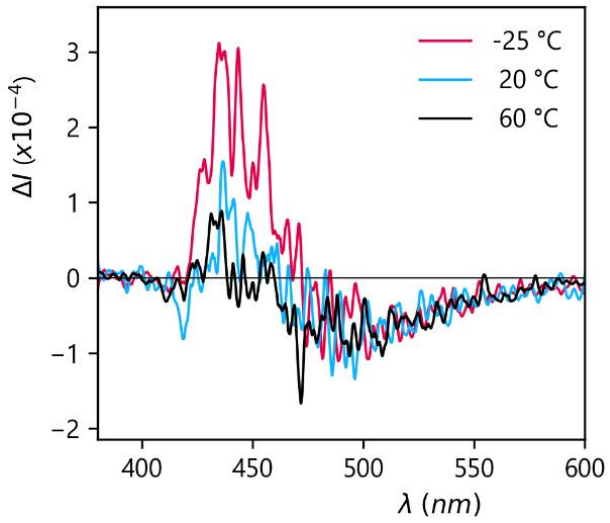

Figure S30: CPL spectra of (*M*)-3 in toluene (10^{-5} M) at three different temperatures

Temperature-dependent CPL measurements support the proposed vibronic-coupling model (Fig. S30). At -25 °C, the g_{lum} value of the nominally "dark" emission band at ~440 nm is significantly enhanced. This behaviour is consistent with reduced thermal activation of low-frequency helicene "breathing" modes (28–40 cm^{-1}), which limits nuclear motion along the coordinate responsible for S_1-S_2 vibronic coupling. Under these conditions, emission predominantly occurs from geometries close to the S_2 minimum, while quenching of the chiroptical signal at ~440 nm through mixing with the oppositely polarised S_1 state is minimized, resulting in an increased CPL response. Upon heating to 60 °C, thermal

population of these low-frequency modes enables broader sampling of the potential energy surface near the S_1/S_2 crossing region, thereby enhancing vibronic mixing between states of opposite rotatory strength. The resulting decrease in g_{lum} at ~440 nm therefore reflects dynamic vibronic averaging rather than simple spectral broadening. Thermally activated oscillations along the breathing coordinate modulate the rotatory strength through Herzberg-Teller-type coupling,[17] leading to partial cancellation of the CPL signal at ~440 nm.

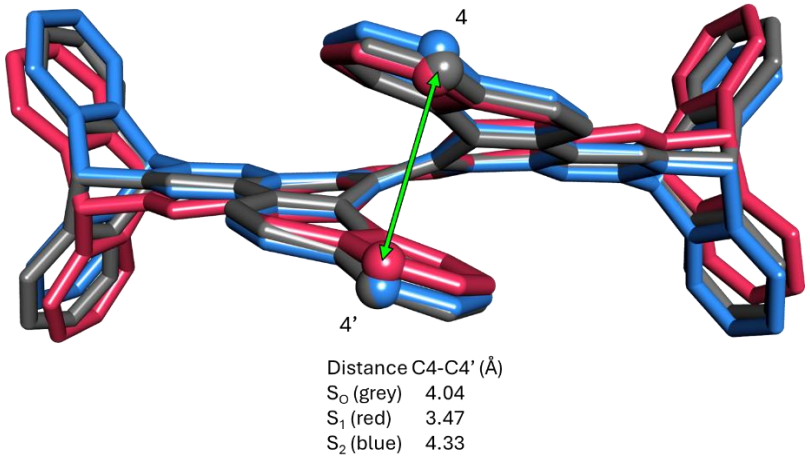

Figure S31: Overlay of the S_0 (DFT B3LYP/cc-pVTZ/GD3), S_1 and S_2 (TD-DFT CAM-B3LYP/cc-pVTZ/GD3) geometries of 3, aligned to the benzene ring at the centre of the helicene backbone

[17] Y. Liu, J. Cerezo, G. Mazzeo, N. Lin, X. Zhao, G. Longhi, S. Abbate and F. Santoro, *J. Chem. Theory Comput.*, 2016, **12**, 2799–2819.

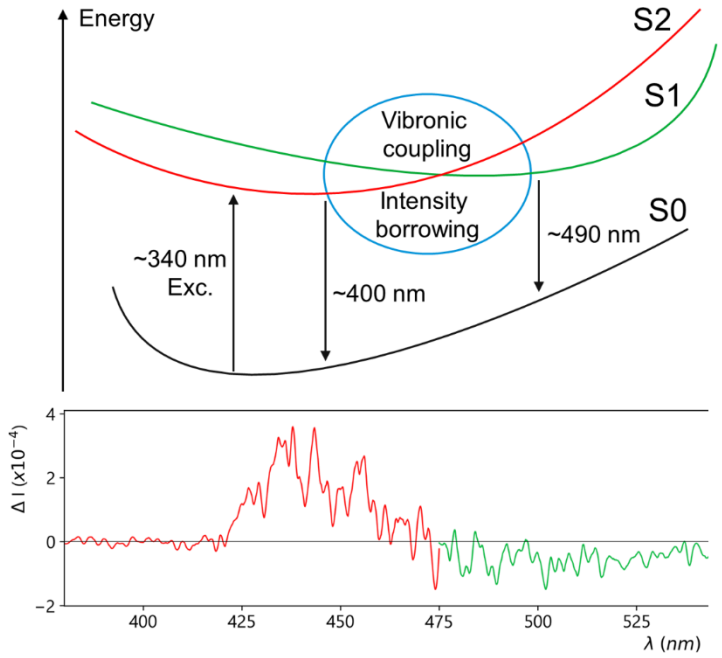

Figure S32: Schematic potential energy surface showing the vibronic coupling between S_1 (B-symmetry, "bright") and S_2 (A-symmetry, "dark") manifolds

The bisignate (dual-band) CPL emission of (*M*)-**3** arises from vibronically coupled S_1 and S_2 excited states. TD-DFT calculations (CAM-B3LYP/cc-pVTZ/GD3) in vacuo identify S_1 (*λ*_calcd. ≈ 489 nm) as a bright B-symmetry π→π* transition (oscillator strength *f* = 0.113, negative rotatory strength *R*), whereas S_2 (λ_calcd. ≈ 386 nm) corresponds to an A-symmetry π→π* manifold with negligible oscillator strength (*f* = 0.001) and positive rotatory strength *R* (Table S4). The low calculated oscillator strength of S_2 likely reflects the absence of explicit solvent-solute interactions in the vacuum model, which can enhance transition dipole moments. The calculated wavelengths and the opposite signs of the rotatory strengths show semi-quantitative agreement with the experimental CPL data. All higher excited states lie too high in energy to be relevant (the five lowest-lying excited states were optimised).

Despite its nominally forbidden character, S_2 becomes emissive through vibronic coupling with S_1 near the crossing region of their potential energy surfaces. Both the S_1 (more "compressed" than the S_0) and S_2 states (more "stretched" than S_0) display significant trans-annular NTOs overlap between the terminal rings, and this electronic proximity in the "compressed" geometry of S_1 promotes strong vibronic coupling with S_2 (*cf*. Fig. 6 and Fig. S31). Low-frequency helicene "breathing" modes (28–40 cm^{-1}) provide the nuclear coordinate that mediates this coupling as the S_1/S_2 PES crossing occurs along the "breathing" mode coordinate, enabling Herzberg–Teller–type intensity borrowing[17] from the bright S_1 state. Consequently, the S_2 emission acquires significant chiroptical activity, producing the higher-energy CPL band. The observed emission from S_2 is consistent with a

vibronically mediated violation of Kasha's rule. The experimentally observed shortening of the S_2 lifetime (7.7 ns) relative to its calculated radiative lifetime (≈2 μs, Table S5) further supports this mechanism.

Temperature-dependent CPL measurements reveal that thermal activation of these low-frequency modes enhances sampling of the S_1/S_2 crossing region, resulting in dynamic vibronic averaging of the CPL signal (Fig. S29). The vibronic coupling is further influenced by the solvent environment and is experimentally more pronounced in THF than in toluene (Fig. 6).

TCSPC Lifetimes

Fluorescence lifetimes of the ditriptycenohelicenes **1**–**3** were determined by TCSPC analysis, revealing that the biexponential decays observed for **1** and **2** (shorter lifetimes ~3–4 ns and longer ones ~10–13 ns) collapse into a clearly monoexponential decay in **3** (single lifetime of ~8 ns), all lifetimes being predictably lower compared to those of non-extended parent helicenes **18**–**20** (Table S5).

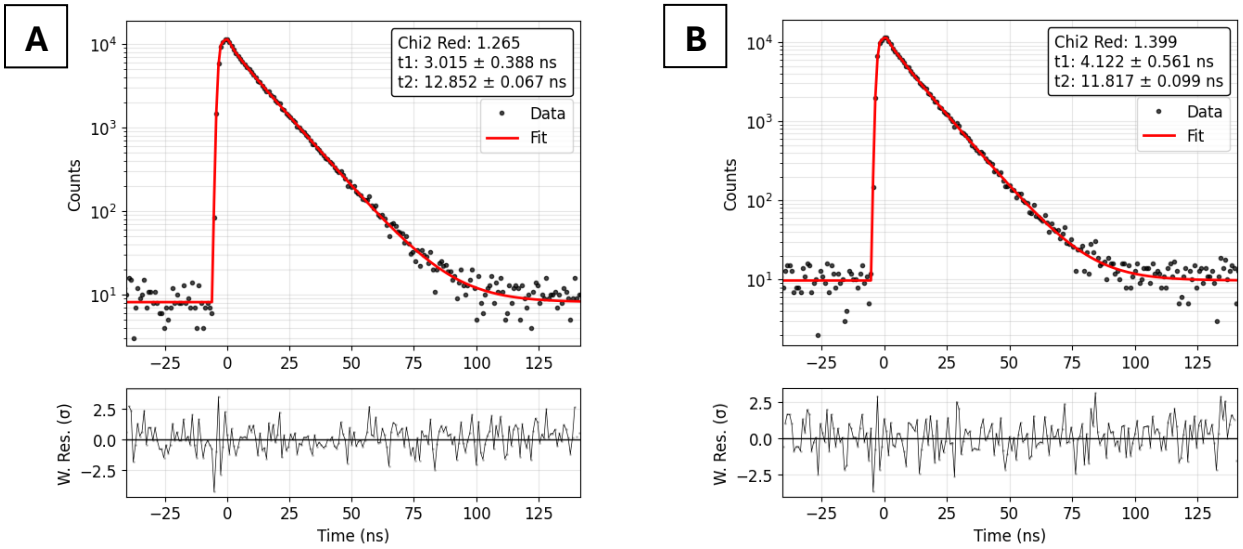

Figure S33: TCSPC histograms of 1 (**A**: 10^{-5} M in THF, **B**: 10^{-5} M in toluene, 420 nm)

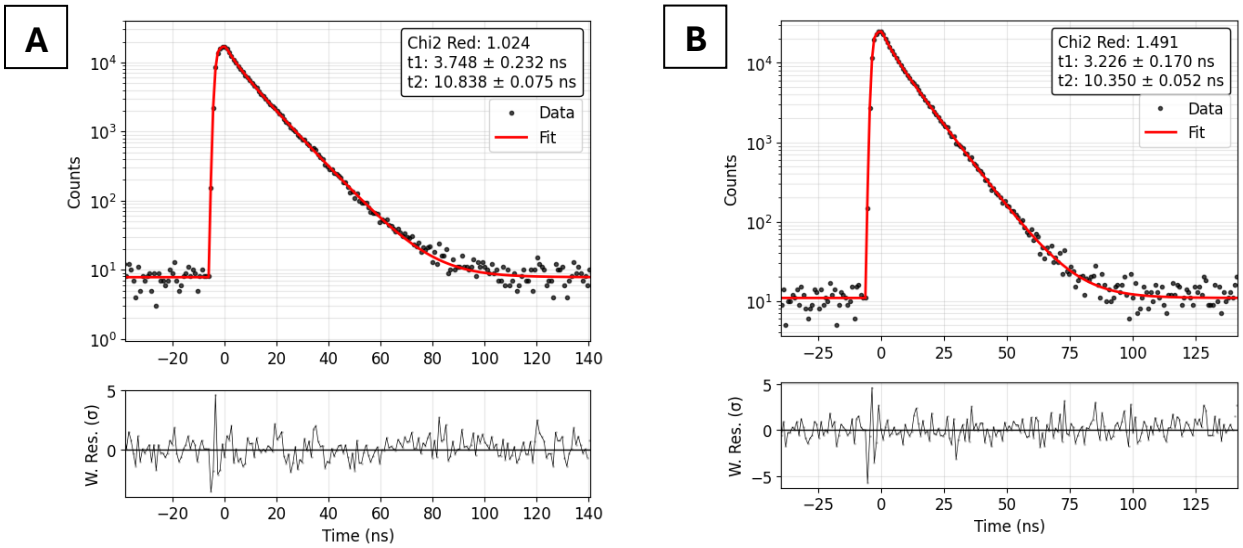

Figure S34: TCSPC histograms of 2 (**A**: 10^{-5} M in THF, **B**: 10^{-5} M in toluene, 420 nm)

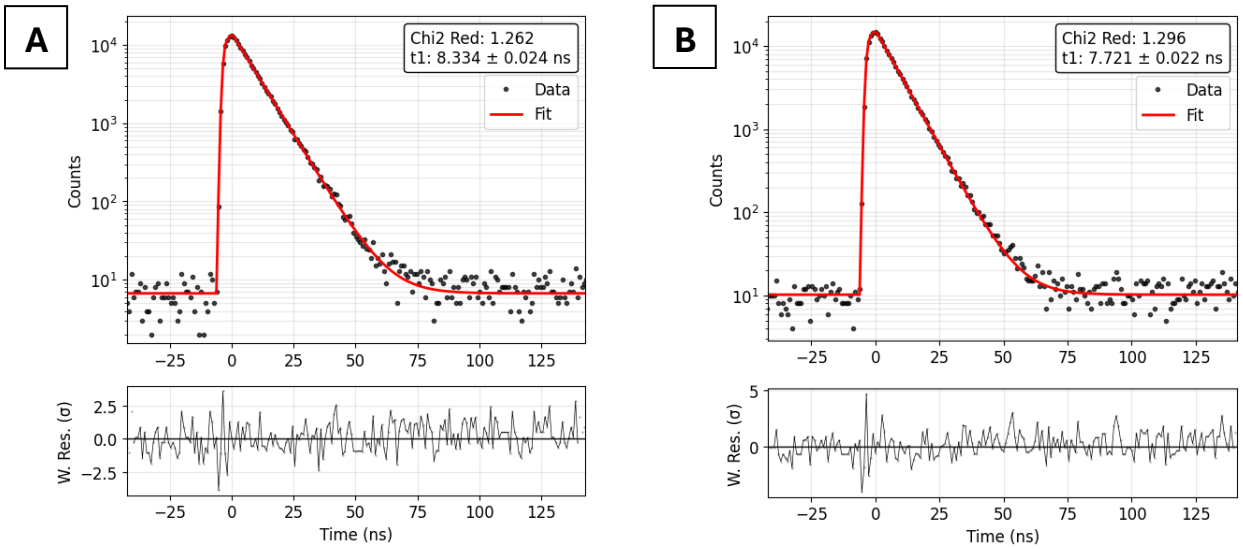

Figure S35: TCSPC histograms of 3 (A: 10^{-5} M in THF, **B**: 10^{-5} M in toluene, 450 nm)

Table S6: Fluorescence lifetimes of racemic ditriptycenohelicenes 1–3 *vs* parent [5]-, [6]- and [7]helicene 18–20

Helicene	Lifetime in THF (ns)[a]	Lifetime in toluene (ns)[a]	Lifetime in dioxane (ns)[b]
1	3.0±0.4 12.85±0.07	4.1±0.6 11.8±0.1	
[5]Helicene 18			25.5
2	3.7±0.2 10.84±0.08	3.2±0.2 10.35±0.05	
[6]Helicene 19			14.5
3	8.33±0.02	7.72±0.02	
[7]Helicene 20			13.8

[a]Determined by TCSPC in THF and toluene (10^{-5} M) at 22 °C. [b]Ref. [18]

[18] J. B. Birks, D. J. S. Birch, E. Cordemans and E. Vander Donckt, *Chem. Phys. Lett.*, 1976, **43**, 33–36.